

Schwinger boson spin liquid states on square lattice

Xu Yang^{*1} and Fa Wang^{1,2}

¹International Center for Quantum Materials, School of Physics, Peking University, Beijing 100871, China

² Collaborative Innovative Center for Quantum Materials, Beijing 100871, China

(Dated: March 3, 2024)

We study possible spin liquids on square lattice that respect all lattice symmetries and time-reversal symmetry within the framework of Schwinger boson (mean-field) theory. Such spin liquids have spin gap and emergent Z_2 gauge field excitations. We classify them by the projective symmetry group method, and find six spin liquid states that are potentially relevant to the J_1 - J_2 Heisenberg model. The properties of these states are studied under mean-field approximation. Interestingly we find a spin liquid state that can go through continuous phase transitions to either the Néel magnetic order or magnetic orders of the wavevector at Brillouin zone edge center. We also discuss the connection between our results and the Abrikosov fermion spin liquids.

PACS numbers: 75.10.Jm, 71.10.Hf

Quantum spin liquid is the ground state of a quantum spin system in two and higher spatial dimensions that does not show any spontaneous symmetry breaking. Since this concept was first introduced four decades ago¹, a lot of theoretical and experimental progress have been made in search for this unconventional phase². In particular several promising experimental candidates have been identified^{2,3}. On the theoretical side, it is understood that quantum spin liquid is more likely to be found in frustrated spin-1/2 models with large classical ground state degeneracy, where strong quantum fluctuations within the degenerate classical ground states may prevent long-range symmetry breaking order⁴.

The square lattice Heisenberg model with nearest-neighbor (J_1) and next-nearest-neighbor (J_2) Heisenberg couplings (abbreviated as J_1 - J_2 model hereafter),

$$H = J_1 \sum_{\langle ij \rangle} \mathbf{S}_i \cdot \mathbf{S}_j + J_2 \sum_{\langle\langle ij \rangle\rangle} \mathbf{S}_i \cdot \mathbf{S}_j, \quad (1)$$

is one of the simplest frustrated spin models. It has attracted a lot of attention for its possible relevance to the copper oxides^{5,6} and iron-based high-temperature superconductors (HTSC)^{7,8}. Ground state of this model is the Néel order [$\langle \mathbf{S}_{(x,y)} \rangle \propto (-1)^{x+y}$] for $J_1 \gg |J_2| \geq 0$ which is the magnetic order of undoped cuprates, or the “stripe” collinear order [$\langle \mathbf{S}_{(x,y)} \rangle \propto (-1)^x$ or $(-1)^y$] for $J_2 \gg |J_1| \geq 0$ which is the magnetic order of many parent compounds of iron-based HTSCs. Spin liquid physics in this model has also been proposed to be relevant to the high temperature superconductivity in these materials⁹⁻¹¹. However it should be noted that the appropriate model for iron-based HTSC is possibly spin-1 (unlike spin-1/2 for cuprates) and may involved biquadratic spin interactions¹². In this paper we will mainly focus on the spin-1/2 case.

The classical ground state of the J_1 - J_2 model at $J_2/J_1 = 1/2$ has large degeneracy. The ground state for quantum spin-1/2 model around $J_2/J_1 = 1/2$ has no magnetic order, although the true nature of this disordered phase has been under debate for a long time¹³⁻¹⁹. Recently a density matrix renormalization group (DMRG) study²⁰ showed evidence of a spin liquid phase with spin gap in the region $0.41 < J_2/J_1 < 0.62$. However a later DMRG result of the same model did not confirm this conclusion²¹. We do not intend to answer whether a spin liquid phase exists in the J_1 - J_2 model. The goal of this paper is to classify spin liquid states within the Schwinger boson formalism, identify candidate states relevant for the J_1 - J_2 and related models and study their properties. It is possible that none of the spin liquid states studied in this paper can be realized in the Heisenberg models on square lattice. Nevertheless they may still be ground state for models close to the J_1 - J_2 model, for example models with ring-exchange interactions.

Spin liquids generically have fractionalized spinon and emergent gauge field excitations^{22,23}. The spinons are spin-1/2 and can be bosonic or fermionic. In this paper we restrict ourselves to the bosonic spinon (Schwinger boson) representation. The spin operators on every site i are expressed by two bosons as

$$\mathbf{S}_i = \frac{1}{2} \sum_{\alpha, \beta = \uparrow, \downarrow} b_{i\alpha}^\dagger \boldsymbol{\sigma}_{\alpha\beta} b_{i\beta}. \quad (2)$$

This enlarges the onsite Hilbert space, a local constraint,

$$\hat{n}_i = \sum_{\alpha} b_{i\alpha}^\dagger b_{i\alpha} = 2S, \quad (3)$$

should be enforced and can be implemented by introducing a $U(1)$ gauge field. In this formalism, spin liquid will have gapped bosonic spinons and boson condensation will produce magnetic orders^{22,24}. In order for this state to be stable in two spatial dimensions (2D), the $U(1)$ gauge field should be gapped, the simplest scenario is to have a spin-singlet spinon pair condensate which reduces

^{*}Current address: Department of Physics, Boston College, Chestnut Hill, Massachusetts 02467, USA

U(1) to Z_2 at low energy by the Higgs mechanism²⁴. Different Z_2 spin liquid phases within this formalism can be described by inequivalent mean-field Hamiltonians, which can be classified by the projective symmetry group method^{27,28}. The mean-field states can be converted to physical spin states by Gutzwiller projection and can in principle be studied numerically by the variational Monte Carlo method²⁹.

This paper is outlined as follows. In Section I, we report the results of PSG analysis for square lattice and the mean-field representation of Z_2 spin liquids which are potentially relevant to the J_1 - J_2 model. We then discuss the properties of these Z_2 spin liquids under mean-field approximation in Section II. Section IV contains further discussion and a summary of results. Technical and numerical details are put in the appendices.

I. PROJECTIVE SYMMETRY GROUP ANALYSIS OF SQUARE LATTICE SCHWINGER BOSON STATES

The projective symmetry group analysis is based on a specific mean-field theory. A mean-field treatment of square lattice Heisenberg model and its PSG analysis using fermionic spinons have been studied by Wen²⁷. In this paper we will study the spin liquid states on square lattice using the Schwinger boson mean-field theory.

With the help of the Schwinger boson representation of the spin operator (2) and SU(2) completeness relation $\sigma_{\alpha\alpha'} \cdot \sigma_{\beta\beta'} = 2\delta_{\alpha\beta'}\delta_{\alpha'\beta} - \delta_{\alpha\alpha'}\delta_{\beta\beta'}$, the Heisenberg interaction can be rewritten as

$$\mathbf{S}_i \cdot \mathbf{S}_j = \hat{B}_{ij}^\dagger \hat{B}_{ij} - \hat{A}_{ij}^\dagger \hat{A}_{ij} \quad (4)$$

where the pairing term $\hat{A}_{ij} = (1/2) \sum_{\alpha,\alpha'} \epsilon_{\alpha\alpha'} b_{i\alpha} b_{j\alpha'}$ and hopping term $\hat{B}_{ij} = (1/2) \sum_{\alpha} b_{i\alpha}^\dagger b_{j\alpha}$ are both SU(2) invariant bond operators.

After a Hubbard-Stratonovich transformation, the quartic terms are decoupled and a mean-field Hamiltonian is obtained:

$$H_{MF} = \sum_{ij} (-A_{ij}^* \hat{A}_{ij} + B_{ij}^* \hat{B}_{ij} + H.c.) + \sum_{ij} (|A_{ij}|^2 - |B_{ij}|^2)/J_{ij} - \mu_i \sum_i (\hat{n}_i - \kappa), \quad (5)$$

where complex numbers $A_{ij} = -A_{ji}$ and $B_{ij} = B_{ji}^*$ are called the mean-field ansatz and the real Lagrangian multiplier μ_i is introduced to enforce the average boson number $\langle \hat{n}_i \rangle \equiv \kappa = 2S$ condition on every site. This mean-field treatment can become a controlled approximation in the large- N limit²⁴⁻²⁶, we will however not pursue this direction.

Minimizing the variational energy with respect to the ansatz A_{ij}, B_{ij} and μ_i yields the self-consistent equations:

$$\langle \hat{n}_i \rangle = \kappa, \quad \langle \hat{A}_{ij} \rangle = A_{ij}/J_{ij}, \quad \langle \hat{B}_{ij} \rangle = B_{ij}/J_{ij}. \quad (6)$$

In the mean-field level, we assume that the Lagrangian multiplier μ_i is independent of site i and the bonds A_{ij} and B_{ij} related by symmetry operations have the same amplitude.

This mean-field theory has an emergent U(1) gauge symmetry, namely that a local gauge transformation

$$b_{j\alpha} \rightarrow e^{i\phi(j)} b_{j\alpha}, \quad \alpha = \uparrow, \downarrow, \quad (7a)$$

$$A_{ij} \rightarrow e^{i[\phi(i)+\phi(j)]} A_{ij}, \quad (7b)$$

$$B_{ij} \rightarrow e^{i[-\phi(i)+\phi(j)]} B_{ij}, \quad (7c)$$

will leave the physical observables unaffected.

The emergent gauge symmetry makes the symmetry of the mean-field ansatz not manifest: a mean-field ansatz after symmetry operation might seem different from the original one, but if they are connected by a gauge transformation the two ansatz still describe the same physical state and hence should be considered identical.

In order to solve this problem, Wen and collaborators suggest that one should use the projective representation of the space group to classify different kinds of mean-field ansatz.

In the projective representation, every symmetry operation X is accompanied by a U(1) gauge transformation G_X ,

$$G_X X(b_{j\alpha}) \rightarrow e^{i\phi_X[X(j)]} b_{X(j)\alpha}. \quad (8)$$

The mean-field ansatz should be invariant under the combined operation $G_X X$ instead of symmetry operation X alone. The collection of all the combined operations which leave the mean-field ansatz invariant form the projective symmetry group (PSG).

Different PSGs characterize different kinds of spin liquid states all sharing the same symmetry. Under certain gauge, the PSG can be fully determined by the commutative relations of the generators of the symmetry group.

The PSG defined through the algebraic relations of the group generators is called the algebraic PSG since there might be PSGs that cannot be realized by any mean-field ansatz.

A. PSG classification of the symmetric spin liquid on square lattice

We set up a rectangular coordinate system and represent the lattice site with two unit vectors \hat{e}_x and \hat{e}_y : $\mathbf{r} = x\hat{e}_x + y\hat{e}_y$, where x, y are integers.

The space group of the square lattice is generated by translation T_1 along \hat{e}_x , translation T_2 along \hat{e}_y , a reflection σ around X-axis and the 90° rotation C_4 around the origin $(x, y) = (0, 0)$.

The action of four generators on a lattice site therefore

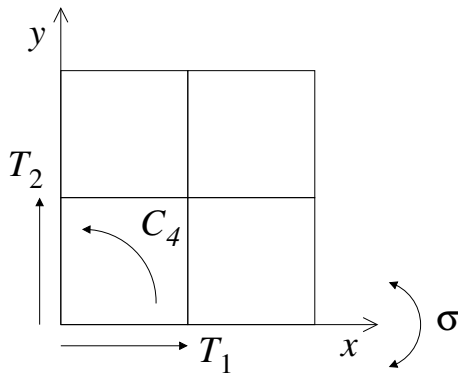


FIG. 1: The coordinate system and space group generators T_1, T_2, C_4, σ of the square lattice.

reads (see also FIG. 1):

$$T_1 : (x, y) \rightarrow (x + 1, y), \quad (9a)$$

$$T_2 : (x, y) \rightarrow (x, y + 1), \quad (9b)$$

$$\sigma : (x, y) \rightarrow (x, -y), \quad (9c)$$

$$C_4 : (x, y) \rightarrow (-y, x). \quad (9d)$$

These generators have the following commutative relations, which completely define the space group,

$$T_1 T_2 = T_2 T_1, \quad (10a)$$

$$T_1 \sigma = \sigma T_1, \quad (10b)$$

$$T_2 \sigma = \sigma T_2^{-1}, \quad (10c)$$

$$\sigma^2 = 1, \quad (10d)$$

$$C_4 \sigma = \sigma C_4^{-1}, \quad (10e)$$

$$C_4^4 = 1, \quad (10f)$$

$$T_1 C_4 = C_4 T_2^{-1}. \quad (10g)$$

Besides the space group generators, we can also add the time-reversal operator \mathcal{T} which is commutative with all the space group generators.

We have solved the algebraic PSG in the Appendix A. Here we will only list the results,

$$\phi_{T_1} = 0, \quad (11a)$$

$$\phi_{T_2} = p_1 \pi x, \quad (11b)$$

$$\phi_{\sigma} = p_2 \pi x + p_3 \pi y + \frac{p_4 \pi}{2}, \quad (11c)$$

$$\phi_{C_4} = p_1 \pi x y + (p_2 + p_3) \pi y + \frac{p_7 \pi}{2}, \quad (11d)$$

$$\phi_{\mathcal{T}} = p_8 \left(x + y - \frac{1}{2} \right) \pi. \quad (11e)$$

where the number $p_1, p_2, p_3, p_4, p_7, p_8$ are numbers which can be either 0 or 1. Therefore there are at most 64 kinds of PSGs.

B. Physical realization of the PSGs on square lattice

Demanding non-vanishing ansatz on certain bonds will impose further constraints on the algebraic PSGs. In Appendix B we have analyzed the constraints imposed on PSGs when demanding an arbitrary non-vanishing bond. Here for simplicity and with the J_1 - J_2 model in mind, we will only report the results for nearest-neighbor (NN) and next-nearest-neighbor (NNN) bonds.

Because of the strong antiferromagnetic J_1 coupling, it is reasonable to assume that the nearest-neighbor pairing ansatz A_1 is nonzero. Under this condition there are two classes of spin liquid states distinguished by the gauge-invariant flux Φ in the elementary plaquette, the zero-flux states with $\Phi = 0$ and the π -flux states with $\Phi = \pi$, where Φ is defined modulo 2π on all plaquettes as³⁰

$$A_{ij}(-A_{jk}^*)A_{kl}(-A_{li}^*) = |A_1|^4 e^{i\Phi}. \quad (12)$$

In the PSG language, the quantum number of flux Φ is p_1 , with zero-flux states corresponding to $p_1 = 0$ and π -flux states corresponding to $p_1 = 1$.

The NN pairing ansatz is invariant under a staggered U(1) gauge transformation, it is necessary to gap out this low energy U(1) gauge field by either nonzero NN hopping B_1 or nonzero NNN pairing A_2 , which will reduce the low energy gauge field to Z_2 ^{22,28}.

The existence of nonzero A_1 demands that $p_2 + p_3 = 1$ and $p_4 = p_2$. Nonzero A_2 requires that $p_1 = 1$ and $p_4 + p_7 = 1$. Nonzero B_1 requires that $p_2 = 0$ and $p_3 = 1$, and that B_1 must be pure imaginary. Nonzero B_2 requires that $p_1 = 0$ and B_2 is real.

The simplest zero-flux Z_2 states can be constructed if we demand the existence of NN pairing A_1 and NN hopping B_1 , with possible existence of NNN hopping B_2 . NNN pairing A_2 is however forbidden in the zero-flux states.

Therefore the PSG for zero-flux states becomes

$$\phi_{T_1} = \phi_{T_2} = 0, \quad (13a)$$

$$\phi_{\sigma} = \pi y, \quad (13b)$$

$$\phi_{C_4} = \pi y + \frac{p_7 \pi}{2}, \quad (13c)$$

$$\phi_{\mathcal{T}} = \left(x + y - \frac{1}{2} \right) \pi. \quad (13d)$$

We are still left with a Z_2 number characterizing two different kinds of spin liquid states. We can further distinguish these two states with the help of another gauge-invariant flux defined on all plaquettes: $\Phi_2 = \text{Arg}[A_{ij}(-A_{jk}^*)(-B_{kl}^*)(-B_{li}^*)]$.

Therefore we obtain two zero-flux ($p_1 = 0$) spin liquid states:

1. $p_7 = 0$, $Z_2[0,0]$ state with fluxes $\Phi_1 = 0$ and $\Phi_2 = 0$ through a plaquette. A_1 and B_2 are real, B_1 is pure

imaginary. The ansatz are given by

$$\begin{aligned} A_{(x,y)(x+1,y)} &= -A_{(x,y)(x,y+1)} = A_1, \\ B_{(x,y)(x+1,y)} &= -B_{(x,y)(x,y+1)} = B_1, \\ B_{(x,y)(x+1,y+1)} &= -B_{(x,y)(x-1,y+1)} = B_2. \end{aligned} \quad (14)$$

2. $p_7 = 1$, $Z_2[0,\pi]$ state with fluxes $\Phi_1 = 0$ and $\Phi_2 = \pi$ through a plaquette. A_1 and B_2 are real, B_1 is pure imaginary. The ansatz are given by

$$\begin{aligned} A_{(x,y)(x+1,y)} &= A_{(x,y)(x,y+1)} = A_1, \\ B_{(x,y)(x+1,y)} &= -B_{(x,y)(x,y+1)} = B_1, \\ B_{(x,y)(x+1,y+1)} &= -B_{(x,y)(x-1,y+1)} = B_2. \end{aligned} \quad (15)$$

We can also obtain π -flux ($p_1 = 1$) states by demanding that A_1 and A_2 are non-vanishing, with possible nonzero B_1 . NNN hopping B_2 is forbidden in π -flux states.

Therefore the PSG for π -flux states becomes

$$\phi_{T_1} = 0, \quad (16a)$$

$$\phi_{T_2} = \pi x, \quad (16b)$$

$$\phi_\sigma = p_2\pi x + (1 - p_2)\pi y + \frac{p_2\pi}{2}, \quad (16c)$$

$$\phi_{C_4} = \pi xy + \pi y + \frac{(1 - p_2)\pi}{2}, \quad (16d)$$

$$\phi_{\mathcal{T}} = p_8(x + y - \frac{1}{2})\pi. \quad (16e)$$

There are four π -flux states depending on the values of p_2 and p_8 . We can further distinguish the four states with gauge-invariant flux $\Phi_3 = \text{Arg}[A_{ij}(-A_{jk}^*)A_{kl}(-A_{li}^*)]$ defined on the triangle $i \rightarrow i + \hat{x} \rightarrow i + 2\hat{x} \rightarrow i + \hat{x} + \hat{y} \rightarrow i$.

Nonzero B_1 can only be realized in the $p_2 = 0$, $p_8 = 1$ state since the coexistence of A_1 and B_1 requires that $p_2 = 0$ and B_1 is pure imaginary.

The NNN pairing A_2 can be real (corresponding to $p_8 = 0$) or pure imaginary ($p_8 = 1$), which is denoted by the letter \mathcal{R} or \mathcal{I} respectively.

Therefore we obtain four π -flux states:

1. $p_2 = 0$, $p_8 = 0$: $Z_2[\pi, 0]\mathcal{R}$ with fluxes $\Phi_1 = \pi$ through the plaquette and $\Phi_3 = 0$ through the triangle. A_1 and A_2 are real.

$$\begin{aligned} (-1)^y A_{(x,y)(x+1,y)} &= A_{(x,y)(x,y+1)} = A_1, \\ (-1)^y A_{(x,y)(x+1,y+1)} &= (-1)^{y+1} A_{(x,y)(x-1,y+1)} = A_2. \end{aligned} \quad (17)$$

2. $p_2 = 0$, $p_8 = 1$: $Z_2[\pi, 0]\mathcal{I}$ with fluxes $\Phi_1 = \pi$ through the plaquette and $\Phi_3 = 0$ through the triangle. A_1 is real and A_2 is pure imaginary. In all four π -flux states B_1 can be nonzero only in this one, and must be pure imaginary.

$$\begin{aligned} (-1)^y A_{(x,y)(x+1,y)} &= A_{(x,y)(x,y+1)} = A_1, \\ (-1)^y A_{(x,y)(x+1,y+1)} &= (-1)^{y+1} A_{(x,y)(x-1,y+1)} = A_2, \\ B_{(x,y)(x+1,y)} &= -B_{(x,y) \rightarrow (x,y+1)} = B_1. \end{aligned} \quad (18)$$

3. $p_2 = 1$, $p_8 = 0$: $Z_2[\pi, \pi]\mathcal{R}$ with fluxes $\Phi_1 = \pi$ through the plaquette and $\Phi_3 = \pi$ through the triangle. A_1 and A_2 are real.

$$\begin{aligned} (-1)^y A_{(x,y)(x+1,y)} &= -A_{(x,y)(x,y+1)} = A_1, \\ (-1)^y A_{(x,y)(x+1,y+1)} &= (-1)^y A_{(x,y)(x-1,y+1)} = A_2. \end{aligned} \quad (19)$$

4. $p_2 = 1$, $p_8 = 1$: $Z_2[\pi, \pi]\mathcal{I}$ with fluxes $\Phi_1 = \pi$ through the plaquette and $\Phi_3 = \pi$ through the triangle. A_1 is real and A_2 is pure imaginary.

$$\begin{aligned} (-1)^y A_{(x,y)(x+1,y)} &= -A_{(x,y)(x,y+1)} = A_1, \\ (-1)^y A_{(x,y)(x+1,y+1)} &= (-1)^y A_{(x,y)(x-1,y+1)} = A_2. \end{aligned} \quad (20)$$

II. MEAN-FIELD THEORY RESULTS

In this section we will study the properties of the two zero-flux states and four π -flux states in the mean-field level.

We will treat the average boson density κ and $\alpha = J_2/J_1$ as variational parameters and obtain the phase diagram of the six states with respect to them.

Since spinons can only be created in pairs, the physical spin excitation spectrum should be the two-spinon continuum spectrum. We compute the lower boundary of the two-spinon spectrum at every given total momentum k for the six spin liquid states, through which we can distinguish different kinds of spin liquid states.

Another measurable quantity is the static spin structure factor. It can be calculated using the formula in the mean-field level:

$$S(\mathbf{k}) = \frac{1}{N_{\text{site}}} \sum_{i,j} \langle \mathbf{S}_i \cdot \mathbf{S}_j \rangle e^{i\mathbf{k} \cdot (\mathbf{r}_i - \mathbf{r}_j)}, \quad (21)$$

where N_{site} is the number of sites.

The two-spinon spin excitation spectrum and static spin structure factor can in principle be measured experimentally by (inelastic) neutron scattering, and numerically by measuring spin-spin correlation functions.

A. Zero-flux state

1. $Z_2[0, 0]$ state

After Fourier transformation $b_{\mathbf{r}} = \frac{1}{\sqrt{N_s}} \sum_{\mathbf{r}} e^{-i\mathbf{k} \cdot \mathbf{r}} b_{\mathbf{k}}$, the mean-field Hamiltonian becomes

$$\begin{aligned} H_{MF} &= \sum_{\mathbf{k}} \Psi_{\mathbf{k}}^\dagger D_{\mathbf{k}} \Psi_{\mathbf{k}} \\ &+ N_s [\mu + \mu\kappa + \frac{2|A_1|^2 - 2|B_1|^2}{J_1} - \frac{2|B_2|^2}{J_2}], \end{aligned} \quad (22)$$

where we have used the Nambu spinor $\Psi_{\mathbf{k}} = (b_{\mathbf{k}\uparrow}, b_{-\mathbf{k}\downarrow}^\dagger)^T$ and the 2×2 matrix

$$D_{\mathbf{k}} = (-2B_2f_1 - \mu)\mathbf{1} - A_1f_-\sigma_y - \text{Im}(B_1)f_-\sigma_z, \quad (23)$$

where $f_1 = \sin(k_x)\sin(k_y)$, $f_{\pm} = \sin(k_x) \pm \sin(k_y)$, $\mathbf{1}$ is the 2×2 identity matrix, $\sigma_{y,z}$ are Pauli matrices.

After a Bogoliubov transformation, the mean-field Hamiltonian can be diagonalized to yield

$$H_{MF} = \sum_{\mathbf{k}} \omega_{\mathbf{k}} (\gamma_{\mathbf{k}\uparrow}^\dagger \gamma_{\mathbf{k}\uparrow} + \gamma_{\mathbf{k}\downarrow}^\dagger \gamma_{\mathbf{k}\downarrow} + 1) + N_s [\mu + \mu\kappa + \frac{2|A_1|^2 - 2|B_1|^2}{J_1} - \frac{2|B_2|^2}{J_2}]. \quad (24)$$

The dispersion relation has two branches ω_{\pm} ,

$$\omega_{\mathbf{k}\pm} = \sqrt{(2B_2f_1 + \mu)^2 - A_1^2f_{\pm}^2} \pm \text{Im}B_1f_{-}. \quad (25)$$

The minima of dispersion are located at $\pm\mathbf{Q}$ where $\mathbf{Q} = (\pi/2, -\pi/2)$, at which points there is an energy splitting between the two branches which is proportional to $|B_1|$.

The self-consistent equations are

$$1 + \kappa = - \int_{BZ} \frac{1}{2} \left[\frac{\partial \omega_{\mathbf{k}+}}{\partial \mu} + \frac{\partial \omega_{\mathbf{k}-}}{\partial \mu} \right] d^2k, \quad (26a)$$

$$4A_1/J_1 = - \int_{BZ} \frac{1}{2} \left[\frac{\partial \omega_{\mathbf{k}+}}{\partial A_1} + \frac{\partial \omega_{\mathbf{k}-}}{\partial A_1} \right] d^2k, \quad (26b)$$

$$4|B_1|/J_1 = \int_{BZ} \frac{1}{2} \left[\frac{\partial \omega_{\mathbf{k}+}}{\partial |B_1|} + \frac{\partial \omega_{\mathbf{k}-}}{\partial |B_1|} \right] d^2k, \quad (26c)$$

$$4B_2/J_2 = \int_{BZ} \frac{1}{2} \left[\frac{\partial \omega_{\mathbf{k}+}}{\partial B_2} + \frac{\partial \omega_{\mathbf{k}-}}{\partial B_2} \right] d^2k. \quad (26d)$$

It can be seen from the dispersion relation Eq. (25) that the ansatz B_1 does not enter the self-consistent equations in the mean-field level. A closer examination also shows that B_1 does not affect the Bogoliubov transformation used to diagonalize the Hamiltonian. But B_1 does have effect on the low-energy effective field theory and magnetic ordered states as we shall see later.

2. $Z_2[0, \pi]$ state

The mean-field Hamiltonian after Fourier transformation becomes:

$$H_{MF} = \sum_{\mathbf{k}} \Psi_{\mathbf{k}}^\dagger D_{\mathbf{k}} \Psi_{\mathbf{k}} + N_s [\mu + \mu\kappa + \frac{2|A_1|^2 - 2|B_1|^2}{J_1} - \frac{2|B_2|^2}{J_2}], \quad (27)$$

where

$$D_{\mathbf{k}} = (-2B_2f_1 - \mu)\mathbf{1} - A_1f_+\sigma_y - \text{Im}(B_1)f_-\sigma_z, \quad (28)$$

The spinon dispersion relations are $\omega_{\mathbf{k}\pm} = \sqrt{(2B_2f_1 + \mu)^2 - A_1^2f_{\pm}^2} \pm \text{Im}(B_1)f_{-}$.

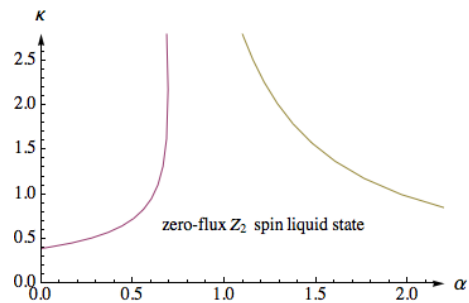


FIG. 2: The mean-field phase diagram for the zero-flux states as a function of ratio $\alpha = J_2/J_1$ and the average boson density κ . The two kinds of zero-flux states cannot be distinguished by their energetics since the NN hopping ansatz B_1 does not enter the mean-field equations. The curves of critical κ_c are plotted. This state has lower energy than the π -flux states in the region where α is relatively low compared to unity. Above the critical value of κ , magnetic order will develop at several k points where the spinon dispersion becomes zero. The magnetic ordered states for the two kinds of zero-flux states are different. The magnetic order obtained from the $Z_2[0, 0]$ state after condensation of boson is the canted Néel order, and the magnetic order from the $Z_2[0, \pi]$ state is the Néel order.

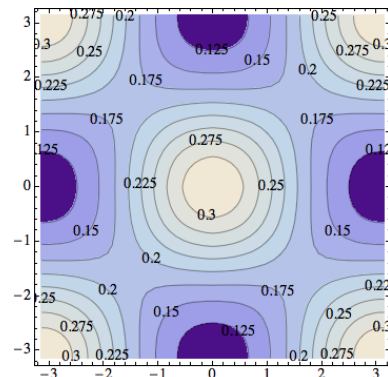


FIG. 3: Static structure factor for the zero-flux state. The spin structure factors for the two zero-flux states are qualitatively similar so here we only show the static structure factor for $Z_2[0, 0]$ state at $\kappa = 0.3$. Axes are k_x and k_y in dimensionless units and the static structure factor is calculated using Eq. (21). The global maxima are located at two wavevectors: $(0, 0)$ and (π, π) . When the phase transition from the zero-flux Z_2 spin liquid states to the magnetic ordered states happens, the Bragg peak will be located at these two wavevectors, which represents the Néel order.

The minima of dispersion are located at $\pm\mathbf{Q}$ where $\mathbf{Q} = (\pi/2, \pi/2)$.

The self-consistent equations are Eq. (26a)-(26d). The bond B_1 serves as the Higgs field to break the $U(1)$ gauge symmetry down to Z_2 . Since B_1 does not enter the self-consistent equations, the two kinds of zero-flux states can not be distinguished by their energy at least in the mean-field level.

We have obtained the phase diagram of the zero-flux

state in FIG. 2, treating average boson density κ and $\alpha = J_2/J_1$ as variational parameters. The curve of critical boson density κ_c is plotted for the zero flux state, above which the energy gap closes and magnetic order is developed.

B. Magnetic order from zero-flux state

In the Schwinger boson formalism, magnetic order is obtained via the condensation of bosons. When boson density κ exceeds critical value κ_c , spinon dispersion will become zero at several \mathbf{Q} points. Bosons will condense at these \mathbf{Q} points and develop magnetic orders.

We have numerically computed the static spin structure factor for the two kinds of zero-flux states and find that there is no qualitative distinction between the two cases. Therefore we only show the static structure factor of the $Z_2[0,0]$ state at a relatively low $\kappa = 0.3$ in Fig. 3. We know from Fig. 3 that the global maxima of the static structure factor are located at $(0,0)$ and (π,π) , which indicates that the spin liquid state is adjacent to the Néel ordered state when the phase transition from the zero-flux Z_2 spin liquid states to the magnetic ordered states happens.

The analytical analysis of magnetic order from $Z_2[0,0]$ and $Z_2[0,\pi]$ states are given in the Appendix C. Here we will report only the final results. For convenience of later discussion, we divide the square lattice into two sublattices, sublattice u for $(-1)^{x+y} = 1$ and sublattice v for $(-1)^{x+y} = -1$.

The magnetic ordered state obtained from the $Z_2[0,0]$ state is a non-collinear order, given by

$$\langle \mathbf{S}(\mathbf{r}) \rangle = \frac{1 + (-1)^{x+y}}{2} \vec{n}_u + \frac{1 - (-1)^{x+y}}{2} \vec{n}_v, \quad (29)$$

where $\vec{n}_{u,v}$ are two vectors of the same length, $|\vec{n}_u| = |\vec{n}_v|$. The angle between \vec{n}_u and \vec{n}_v are in general less than 180° unless $B_1 = 0$. This represents the ‘‘canted Néel order’’, which is the classical ground state for nearest-neighbor Heisenberg model under a small uniform magnetic field.

Aside from the spin (magnetic dipole) order parameter $\vec{n}_{u,v}$, this canted Néel order also has another vector spin chirality order parameter

$$\vec{C}_{ij} = \nu_{ij} \langle \mathbf{S}_i \times \mathbf{S}_j \rangle, \quad (30)$$

where $\nu_{ij} = \pm 1$ on the nearest neighbor bond $\langle ij \rangle$, and takes value $+1(-1)$ if site i belongs to sublattice $u(v)$.

The magnetic order obtained from the $Z_2[0,\pi]$ state is the collinear Néel order, $\langle \mathbf{S}(\mathbf{r}) \rangle = (-1)^{x+y} \vec{n}$. But this state is not the conventional Néel order and will also acquire a nonzero ground state expectation value of the vector spin chirality order parameter $\langle \mathbf{S}_i \times \mathbf{S}_j \rangle$ due to quantum fluctuations.

In the effective field theory, the transition from Z_2 spin liquid state to the magnetic ordered state occurs

through the condensation of the charge-1 [in terms of the emergent U(1) gauge field] spinon field z_α . B_1 serves as a charge-‘‘-2’’ Higgs field. The physical observables are charge-‘‘0’’ combinations of the spinon field z_α . The three possible bilinear combinations are as follows:

$$\vec{n}_1 = z^\dagger \vec{\sigma} z, \quad \vec{n}_2 = \text{Re}[B_1 z^T i \sigma^y \vec{\sigma} z], \quad \vec{n}_3 = \text{Im}[B_1 z^T i \sigma^y \vec{\sigma} z], \quad (31)$$

which are orthogonal to each other.

It is easy to see that \vec{n}_1 can be identified with Néel order parameter. And since the vector spin chirality order parameter is even under time-reversal transformation, we can identify it with $\text{Re}[B_1 z^T i \sigma^y \vec{\sigma} z]$. The order parameter is in fact the triad $\vec{n}_{1,2,3}$, even if the expectation values of spins form the collinear Néel order. This kind of magnetic order has been obtained before on honeycomb lattice in proximity to certain spin liquid state³¹.

C. Critical field theory for transition from zero-flux spin liquid states to magnetic order

When κ exceeds the critical value κ_c , there will be a phase transition from the Z_2 spin liquid state into the magnetic ordered state. Close to the phase transition point a continuous field theory can be derived.

The low-energy effective Lagrangian for the transition from $Z_2[0,0]$ state to the canted Néel order reads

$$\begin{aligned} \mathcal{L} = \int d^2\mathbf{r} \{ & \frac{8}{(-\mu + 2A_1 + 2B_2)a^2} \text{Im}(B_1) \omega_\alpha^* \frac{d}{d\tau} \omega_\alpha \\ & + (A_1 - 2B_2 + \frac{4|B_1|^2}{-\mu + 2A_1 + 2B_2}) \partial_{\mathbf{r}} \omega_\alpha^* \cdot \partial_{\mathbf{r}} \omega_\alpha \\ & + (\frac{-2\mu - 4A_1 + 4B_2}{a^2} - \frac{8|B_1|^2}{(-\mu + 2A_1 + 2B_2)a^2}) \omega_\alpha^* \omega_\alpha \}, \end{aligned} \quad (32)$$

where ω is related to the spinon field z and is defined in Eq. (D10). Summation over repeated indices is implied hereafter.

The coefficient of the mass term $\omega_\alpha^* \omega_\alpha$ will change sign upon approaching the critical point, indicating that the critical chemical potential is $\mu \rightarrow 2B_2 - \sqrt{4A_1^2 + 4|B_1|^2}$. The low-energy effective field theory now flows to a fixed point where space and time scales differently with dynamical critical exponent $z = 2$, which is different from previous theories of such phase transitions²². By power counting one can find that this theory approaches the upper critical dimension $d = 4$ where the physics is controlled by a Gaussian fixed point and the fluctuation around the mean-field theory is negligible. The scaling properties of correlation functions can be determined by naive power counting since in the upper critical dimension, the anomalous dimension correction approaches zero in the $4 - \epsilon$ analysis when $\epsilon \rightarrow 0$. For example, $\langle \mathbf{S}(0) \cdot \mathbf{S}(\mathbf{r}) \rangle \propto |\mathbf{r}|^{-\eta}$, where η is 4 plus correction which is proportional to ϵ and hence is negligible.

The low-energy effective Lagrangian for the transition from $Z_2[0, \pi]$ state to the Néel ordered state is

$$\mathcal{L} = \int d^2\mathbf{r} \{ |D_\tau z|^2 + c^2 |D_{\mathbf{r}} z|^2 + m^2 |z|^2 \}. \quad (33)$$

The couplings between Higgs and spinon fields have at least two spatial derivatives and one time derivative, which is irrelevant by naive power counting. Anomalous dimension will not change this result. Upon approaching the critical point, the mass term will disappear and this theory has an enlarged $O(4)$ symmetry. The scaling properties of the field theory at $O(4)$ critical point have been studied both analytically and numerically. The scaling behaviour of the correlation functions is therefore known. As an example, the spin-spin correlation function has a relatively large anomalous dimension, which behaves as $\langle \mathbf{S}(0) \cdot \mathbf{S}(\mathbf{r}) \rangle \propto |\mathbf{r}|^{-\eta}$, where η is numerically determined as $\eta = 1.373(3)$ in contrast to the result for $Z_2[0, 0]$ state³².

The transformation rules for spinon fields (ω or z) under space-group symmetry can also be readily deduced from the PSG and are listed in TABLE I. It is easy to verify that the form of Lagrangian is invariant under these transformation rules.

$Z_2[0, 0]$ state	$Z_2[0, \pi]$ state	Symmetry Operation
$\omega \rightarrow -i\omega$	$z \rightarrow -i\sigma^y z^*$	T_1
$\omega \rightarrow i\omega$	$z \rightarrow i\sigma^y z^*$	T_2
$\omega \rightarrow \omega$	$z \rightarrow z$	C_4
$\omega \rightarrow \omega$	$z \rightarrow z$	σ
$\omega \rightarrow \omega$	$z \rightarrow \sigma^y z^*$	\mathcal{T}

TABLE I: Transformation rules of the spinon fields under PSG.

D. π -flux state

1. $Z_2[\pi, 0]\mathcal{R}$ state

There are two sites in a unit cell of π -flux ansatz distinguished by $(-1)^y = \pm 1$ which can be labeled by u and v respectively. The unit cells are labeled by integers x and \tilde{y} , where the $u(v)$ site in the unit cell at (x, \tilde{y}) are at position $(x, y) = (x, 2\tilde{y})$ [$(x, y) = (x, 2\tilde{y} + 1)$].

After Fourier transformation

$$b_{(u,v)\mathbf{r}\alpha} = \frac{1}{\sqrt{N_s}} \sum_{x,\tilde{y}} e^{-i(k_x x + 2k_y \tilde{y})} b_{(u,v)\mathbf{k}\alpha}, \quad (34)$$

where $k_{x,y} \equiv \mathbf{k} \cdot \mathbf{e}_{x,y}$, the mean-field Hamiltonian becomes:

$$H_{MF} = \sum_{\mathbf{k}} \Psi_{\mathbf{k}}^\dagger D_{\mathbf{k}} \Psi_{\mathbf{k}} + N_s [\mu + \mu\kappa + 2|A_1|^2/J_1 + 2|A_2|^2/J_2], \quad (35)$$

in which,

$$D_{\mathbf{k}} = \begin{pmatrix} \mu \cdot 1 & A_1 P_1 + A_2 P_2 \\ -A_1 P_1 - A_2^* P_2 & \mu \cdot 1 \end{pmatrix}.$$

And we have also used the Nambu spinor

$$\Psi_i = \begin{pmatrix} b_{u\mathbf{k}\uparrow} \\ b_{v\mathbf{k}\uparrow} \\ b_{u-\mathbf{k}\downarrow}^\dagger \\ b_{v-\mathbf{k}\downarrow}^\dagger \end{pmatrix}$$

and two 2×2 antihermitian matrices

$$P_1 = \frac{1}{2} \begin{pmatrix} 2i\sin(k_x) & -1 + e^{2ik_y} \\ 1 - e^{-2ik_y} & -2i\sin(k_x) \end{pmatrix}, \quad (36)$$

$$P_2 = \frac{1}{2} \begin{pmatrix} 0 & -\xi_{\mathbf{k}}^* \\ \xi_{\mathbf{k}} & 0 \end{pmatrix}, \quad (37)$$

where $\xi_{\mathbf{k}} = e^{ik_x} - e^{-ik_x} + e^{-i(k_x+2k_y)} - e^{i(k_x-2k_y)}$.

The Hamiltonian can be diagonalized by a Bogoliubov transformation using a $SU(2,2)$ matrix to yield :

$$H_{MF} = \sum_{\mathbf{k}; a=u,v} \omega_{\mathbf{k}} (\gamma_{a\mathbf{k}\uparrow}^\dagger \gamma_{a\mathbf{k}\uparrow} + \gamma_{a\mathbf{k}\downarrow}^\dagger \gamma_{a\mathbf{k}\downarrow} + 1) + N_s [\mu + \mu\kappa + 2|A_1|^2/J_1 + 2|A_2|^2/J_2]. \quad (38)$$

In this state A_2 is real, the dispersion relation is therefore fourfold degenerated:

$$\omega_{\mathbf{k}} = \sqrt{\mu^2 - A_1^2 f_1 - 4A_2^2 f_2}, \quad (39)$$

where $f_1 = \sin^2(k_x) + \sin^2(k_y)$, $f_2 = \sin^2(k_x)\sin^2(k_y)$.

The minima of spinon dispersion are located at $(k_x, k_y) = \pm(\pi/2, \pi/2)$.

The mean-field self-consistent equations are as follows:

$$1 + \kappa = - \int_{BZ} \frac{\partial \omega_{\mathbf{k}}}{\partial \mu} d^2 k, \quad (40a)$$

$$4A_1/J_1 = - \int_{BZ} \frac{\partial \omega_{\mathbf{k}}}{\partial A_1} d^2 k, \quad (40b)$$

$$4A_2/J_2 = - \int_{BZ} \frac{\partial \omega_{\mathbf{k}}}{\partial A_2} d^2 k. \quad (40c)$$

Solving the self-consistent equations we have obtained a mean-field phase diagram for this state as shown in FIG. 4. This state has $\kappa_c \approx 0.81$ but exist in the regime $\alpha = J_2/J_1 \approx 0.75 \sim 1$ far away from the physically interesting regime $\alpha \approx 0.5$. Therefore this state is unlikely to be the physical ground state for the square lattice $J_1 - J_2$ Heisenberg model found in the numerical methods. The lower edge of the two-spinon spectrum is displayed in Fig. 5 for the $Z_2[\pi, 0]\mathcal{R}$ state at $\kappa = 0.5$, which could be used as a probe for this state in numerical simulations.

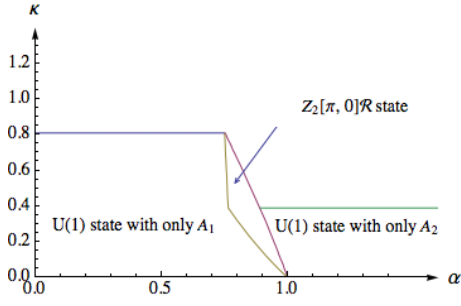


FIG. 4: The mean-field phase diagram for the $Z_2[\pi, 0]\mathcal{R}$ π -flux state as a function of ratio $\alpha = J_2/J_1$ and the average boson density κ . This state has a critical value of $\kappa \approx 0.81$, and occupy a finite area in the regime $\alpha = J_2/J_1 \approx 0.75 \sim 1$. Upon decreasing the value of α , the Z_2 spin liquid state will become a U(1) spin liquid state with only non-zero nearest-bond A_1 through a first-order phase transition. The U(1) spin liquid state with only A_1 has a critical value of $\kappa \approx 0.81$. Upon increasing the value of α , the Z_2 spin liquid state will become a U(1) spin liquid state with only non-zero A_2 through a first-order phase transition. The U(1) spin liquid state with only A_2 can be regarded as two copies of decoupled π -flux states on the square lattice and has a critical value of $\kappa \approx 0.40$.

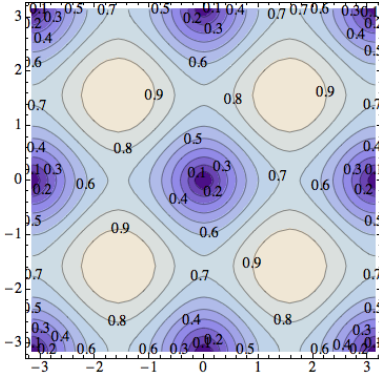


FIG. 5: The lower edge of the two-spinon spectrum for the $Z_2[\pi, 0]\mathcal{R}$ state at $\kappa = 0.81$.

2. $Z_2[\pi, 0]\mathcal{I}$ state

This state has nonzero B_1 , so after Fourier transformation, the Hamiltonian becomes

$$H_{MF} = \sum_{\mathbf{k}} \Psi_{\mathbf{k}}^\dagger \begin{pmatrix} \mu \cdot 1 + B_1 P_3 & A_1 P_1 + A_2 P_2 \\ -A_1 P_1 - A_2^* P_2 & \mu \cdot 1 - B_1 P_3 \end{pmatrix} \Psi_{\mathbf{k}}. \quad (41)$$

In this state A_2 is pure imaginary, we have two twofold-degenerate dispersion :

$$\omega_{\mathbf{k}\pm} = \sqrt{\mu^2 - (A_1^2 - |B_1|^2)f_1 - 4|A_2|^2 f_2 \pm 2\sqrt{(|B_1|^2 + 4(A_1^2 - |B_1|^2)|A_2|^2 f_2)} f_1}, \quad (42)$$

where $f_1 = \sin^2(k_x) + \sin^2(k_y)$, $f_2 = \sin^2(k_x)\sin^2(k_y)$ and

$$P_3 = \frac{1}{2} \begin{pmatrix} 2i\sin(k_x) & -1 + e^{2ik_y} \\ 1 - e^{-2ik_y} & -2i\sin(k_x) \end{pmatrix}, \quad (43)$$

Minima of the spinon dispersion are at $(k_x, k_y) = \pm(\pi/2, \pi/2)$.

The self-consistent equations are as follows:

$$1 + \kappa = - \int_{BZ} \frac{1}{2} \left[\frac{\partial \omega_{\mathbf{k}+}}{\partial \mu} + \frac{\partial \omega_{\mathbf{k}-}}{\partial \mu} \right] d^2 k, \quad (44a)$$

$$4A_1/J_1 = - \int_{BZ} \frac{1}{2} \left[\frac{\partial \omega_{\mathbf{k}+}}{\partial A_1} + \frac{\partial \omega_{\mathbf{k}-}}{\partial A_1} \right] d^2 k, \quad (44b)$$

$$4|B_1|/J_1 = + \int_{BZ} \frac{1}{2} \left[\frac{\partial \omega_{\mathbf{k}+}}{\partial |B_1|} + \frac{\partial \omega_{\mathbf{k}-}}{\partial |B_1|} \right] d^2 k, \quad (44c)$$

$$4|A_2|/J_2 = - \int_{BZ} \frac{1}{2} \left[\frac{\partial \omega_{\mathbf{k}+}}{\partial |A_2|} + \frac{\partial \omega_{\mathbf{k}-}}{\partial |A_2|} \right] d^2 k. \quad (44d)$$

The self-consistent equations are Eq. (40a)-(40c). The mean-field phase diagram for the $Z_2[\pi, 0]\mathcal{I}$ state is obtained as shown in FIG. 6. This state has a relatively low κ_c . The lower edge of the two-spinon spectrum is displayed in Fig. 7 for the $Z_2[\pi, 0]\mathcal{I}$ state at $\kappa = 0.6$.

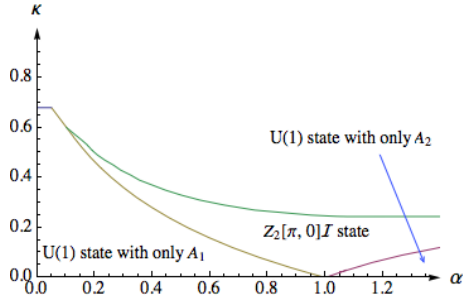


FIG. 6: The mean-field phase diagram for the $Z_2[\pi, 0]\mathcal{I}$ π -flux state as a function of ratio $\alpha = J_2/J_1$ and the average boson density κ . This state has a critical value of $\kappa \approx 0.60$, and occupy a finite area in the regime $\alpha > 0.10$.

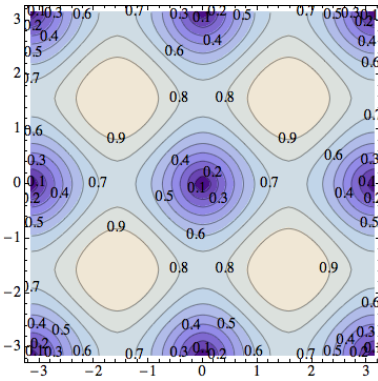


FIG. 7: The lower edge of the two-spinon spectrum for the $Z_2[\pi, 0]\mathcal{I}$ state at $\kappa = 0.60$.

3. $Z_2[\pi, \pi]\mathcal{R}$ state

The Hamiltonian after Fourier transformation is now (up to a constant):

$$H_{MF} = \sum_{\mathbf{k}} \Psi_{\mathbf{k}}^\dagger \begin{pmatrix} \mu \cdot 1 & A_1 P_1 + A_2 P_2 \\ -A_1 P_1 - A_2^* P_2 & \mu \cdot 1 \end{pmatrix} \Psi_{\mathbf{k}}. \quad (45)$$

And we have used two 2×2 matrices:

$$P_1 = \frac{1}{2} \begin{pmatrix} 2i\sin(k_x) & 1 - e^{2ik_y} \\ -1 + e^{-2ik_y} & -2i\sin(k_x) \end{pmatrix}, \quad (46)$$

$$P_2 = \frac{1}{2} \begin{pmatrix} 0 & -\xi_{\mathbf{k}}^* \\ \xi_{\mathbf{k}} & 0 \end{pmatrix}, \quad (47)$$

where $\xi_{\mathbf{k}} = e^{ik_x} + e^{-ik_x} + e^{-i(k_x+2k_y)} + e^{i(k_x-2k_y)}$.

The dispersion relation is fourfold degenerate:

$$\omega = \sqrt{\mu^2 - A_1^2 f_1 - 4A_2^2 f_2}, \quad (48)$$

where $f_1 = \sin^2(k_x) + \sin^2(k_y)$, $f_2 = \cos^2(k_x)\cos^2(k_y)$.

We denote $|A_2|/A_1 = \tan(\theta)$. When $\theta < \arctan(1/\sqrt{2})$, the minima are located at $\pm(\pi/2, \pi/2)$, and when $\theta > \arctan(1/\sqrt{2})$, the minima jump to $(k_x, k_y) = (0, 0)$ and $(\pi, 0)$.

The curve of critical κ is obtained via the self-consistent equation as shown in FIG. 8. This state has a relatively high value of $\kappa_c \approx 1.36$ even above the physical value $\kappa = 1$. Close to the physically interesting regime where $\kappa = 1$ and $\alpha = J_2/J_1 \approx 0.5$, this state occupy a finite area of phase space, and hence might be a promising candidate for the numerically found Z_2 spin liquid state. But a closer study shows that this state is energetically more unfavorable than the $Z_2[\pi, \pi]\mathcal{I}$ state in the physically interesting regime. The lower edge of the two-spinon spectrum is displayed in Fig. 9 for the $Z_2[\pi, \pi]\mathcal{R}$ state at $\kappa = 1.36$.

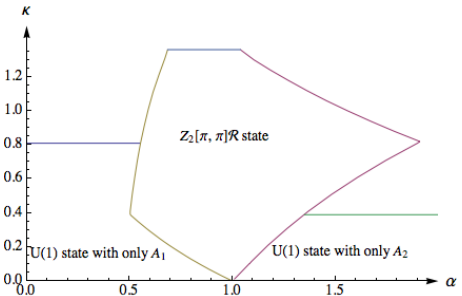


FIG. 8: The mean-field phase diagram for the $Z_2[\pi, \pi]\mathcal{R}$ π -flux state as a function of ratio $\alpha = J_2/J_1$ and the average boson density κ . This state has a critical value of $\kappa \approx 1.36$, and occupy a finite area in the regime $\alpha = J_2/J_1 \approx 0.5 \sim 1.9$.

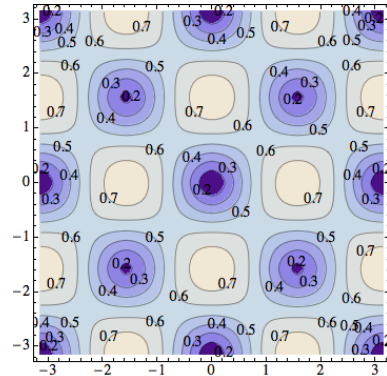


FIG. 9: The lower edge of the two-spinon spectrum for the $Z_2[\pi, \pi]\mathcal{R}$ state at $\kappa = 1.36$.

4. $Z_2[\pi, \pi]\mathcal{I}$ state

The mean-field Hamiltonian is Eq. (45).

In this state, A_2 is imaginary, so the dispersion relations are twofold degenerated:

$$\omega_{\pm} = \sqrt{\mu^2 - A_1^2 f_1 - 4|A_2|^2 f_2 \pm 4A_1|A_2|\sqrt{f_1 f_2}} \quad (49)$$

where $f_1 = \sin^2(k_x) + \sin^2(k_y)$, $f_2 = \cos^2(k_x)\cos^2(k_y)$.

Define $|A_2|/A_1 = \tan(\theta)$. When $\theta < \arctan(1/(2\sqrt{2}))$, the minima are at $(k_x, k_y) = \pm(\pi/2, \pi/2)$. When $\theta > \arctan(1/(2\sqrt{2}))$, the minima will move to incommensurate wave vectors $(k_x, k_y) = \pm(q, q)$, where $\sin(q) = 1/(2\sqrt{2}\tan(\theta))$.

The self-consistent equations are Eq. (44a)-(44d) and the mean-field phase diagram is obtained as shown in FIG. 10.

This state has a high $\kappa_c \approx 1.62$ even above the physical value $\kappa = 2S = 1$ and occupy a finite area of phase diagram close to the physically interesting regime $\kappa \approx 1$ and $\alpha \approx 0.5$. Although this state is energetically more unfavorable than the zero-flux states in this regime, we propose that by adding ring-exchange term in the Hamiltonian may favor the π -flux spin liquid state. The lower edge of the two-spinon spectrum is displayed in Fig. 11 for the $Z_2[\pi, \pi]\mathcal{I}$ state at $\kappa = 1.62$.

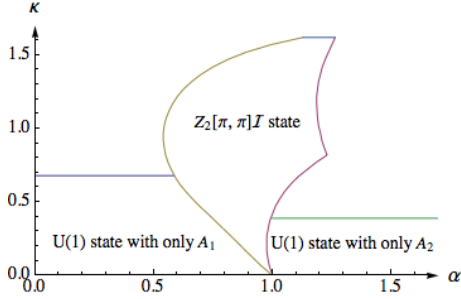


FIG. 10: The mean-field phase diagram for the $Z_2[\pi, \pi]\mathcal{I}$ π -flux state as a function of ratio $\alpha = J_2/J_1$ and the average boson density κ . This state has a critical value of $\kappa \approx 1.62$, and occupy a finite area in the regime $0.55 < \alpha < 1.27$.

E. Magnetic order from π -flux states

We have computed the static spin structure factor for the four kinds of π -flux states in the mean-field level and find that there is no qualitative distinction between these four cases. Therefore we only show the static structure factor of the $Z_2[\pi, 0]\mathcal{R}$ state at a relatively low $\kappa = 0.2$ in FIG. 12. From Fig. 12 that the global maxima of the static structure factor are located at $\pm(\pi, 0)$ and $\pm(0, \pi)$, which indicates that the magnetic ordered state adjacent to the π -flux state is different from the Néel order.

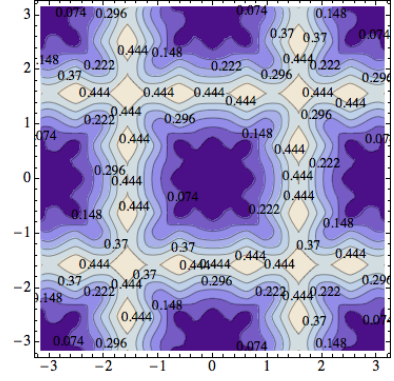


FIG. 11: The lower edge of the two-spinon spectrum for the $Z_2[\pi, \pi]\mathcal{I}$ state at $\kappa = 1.62$.

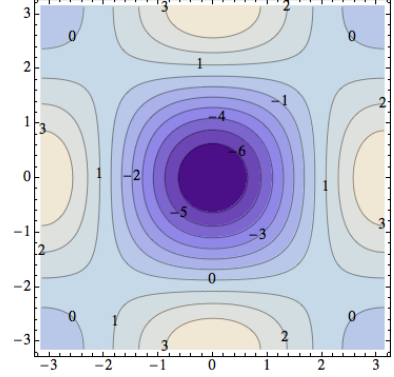


FIG. 12: Spin structure factor for the π -flux state. The spin structure factors for the four π -flux states are qualitatively the same so here we only show the static structure factor for $Z_2[\pi, 0]\mathcal{R}$ state at $\kappa = 0.2$. Axes are in dimensionless units k_x and k_y and the static structure factor is calculated using Eq. 21. The global maxima are located at four wave vectors $\pm(\pi, 0)$ and $\pm(0, \pi)$. It is expected that when the continuum phase transition from the π -flux Z_2 spin liquid states to the magnetic ordered states happens, the Bragg peak will located at these four wave vectors, which represents a new kind of magnetic order different from the Néel order.

We have also analytically obtained the magnetic ordered state starting from the mean-field Hamiltonian using the method of boson condensation. For simplicity, we shall only consider a π -flux state which only has NN bond A_1 . The mean-field Hamiltonian after Fourier transformation is

$$H_{MF} = \sum_{\mathbf{k}} \Psi_{\mathbf{k}}^{\dagger} \begin{pmatrix} \mu \cdot 1, & A_1 P_1 \\ -A_1 P_1, & \mu \cdot 1 \end{pmatrix} \Psi_{\mathbf{k}}, \quad (50)$$

where

$$P_1 = \frac{1}{2} \begin{pmatrix} 2i\sin(k_x), & -1 + e^{2ik_y} \\ 1 - e^{-2ik_y}, & -2i\sin(k_x) \end{pmatrix}. \quad (51)$$

The critical spinon vector occurs at two inequivalent \mathbf{k} points $\pm\mathbf{Q}$, where $\mathbf{Q} = (\pi/2, \pi/2)$.

Under the constraint that the density of condensate on every lattice site is uniform, we can work out the pattern of spinon condensation.

We then find a set of four-sublattice ordered states consistent with a subset of the classical ground state for $J_2/J_1 = 1/2$ Heisenberg model.

The magnetic order is $\langle S(\mathbf{r}) \rangle = \mathbf{m}_1(-1)^x + \mathbf{m}_2(-1)^y + \mathbf{m}_3(-1)^{x+y}$, where $\mathbf{m}_{1,2,3}$ are three orthogonal vectors and

$$m_1^2 + m_2^2 + m_3^2 = m^2. \quad (52)$$

Technical details of the calculation can be found in the Appendix C 3.

III. DUALITY BETWEEN SCHWINGER BOSON SPIN LIQUID STATES AND ABRIKOSOV FERMION SPIN LIQUID STATES

In the parton constructions of the Heisenberg model, the physical spin operator can be decomposed into spin-1/2 partons that can be either bosonic (Schwinger bosons) or fermionic (Abrikosov fermions). Whether the two seemingly distinct approaches are equivalent or not remains a long-standing puzzle. In this section we closely follow the work of Hermele *et al.*³³ and Lu *et al.*³⁴ and deduce the correspondence between the PSGs of the Schwinger boson representation and Abrikosov fermion representation.

We know clearly from the PSG classification of spin liquid states that topological order alone is not enough to fully characterize the different phases of the spin liquid states when symmetry is also presented³³. Actually, the interplay of topological order and symmetry will yield a richer structure called the ‘‘symmetry enriched topological order’’^{27,28,33,35–38}. In different symmetry enriched topological phases, anyon excitations will not only have fractional charges and fractional statistics, but also carry fractional symmetry quantum numbers. To be more concrete, the symmetry operation acts on anyons projectively and when an anyon returns to its original position after a series of symmetry operation, it may gain a nontrivial phase factor due to the gauge structure of the theory. All the fractionalization of symmetry quantum numbers of a certain type of anyon put together defines a fractionalization class for this type of anyon. In the case of Schwinger boson spin liquid states, the fractional symmetry quantum numbers p_i ($i = 1, 2, 3, 4, 7, 8$) fully determine the fractionalization class for the bosonic spinon. Once the fractionalization classes for each type of anyon excitations of a topological ordered state is determined, we can specify a symmetry class for this kind of symmetry enriched topological phase.

The fusion rules between different types of anyons have certain constraints on the fractionalization classes in the same symmetry class. Therefore we could use the compatibility condition to determine the correspondence between the fermionic PSGs and bosonic PSGs.

In the present case, three kinds of topological excitations, bosonic spinon b , fermionic spinon f and the vison v , obey the following fusion rules.

$$\begin{aligned} b \times f &= v, \quad b \times v = f, \quad f \times v = b, \\ b \times b &= f \times f = v \times v = 1. \end{aligned} \quad (53)$$

The fusion rules have a strong constraints on the symmetry fractionalization between the three kinds of topological excitations. Therefore in principle we could obtain the vison PSG from the knowledge of the fermionic PSG and the bosonic PSG due to the fusion rule $b \times v = f$. The additional phase $e^{i\phi_f}$ picked up by a fermion can be obtained from the phase $e^{i\phi_b}$ of a boson, the phase $e^{i\phi_v}$ of a vison, and possibly a twist factor $e^{i\phi_t}$ from the mutual statistics of bosons and visons, therefore we have

$$e^{i\phi_f} = e^{i\phi_v} \cdot e^{i\phi_b} \cdot e^{i\phi_t}. \quad (54)$$

Algebraic Identities	bosonic b_α	fermionic f_α	vison $v = b \times f$
$T_2^{-1}T_1T_2T_1^{-1}$	$(-1)^{p_1}$	η_{xy}	-1
$\sigma^{-1}T_1\sigma T_1^{-1}$	$(-1)^{p_2}$	η_{xpy}	-1
$\sigma^{-1}T_2\sigma T_2$	$(-1)^{p_3}$	η_{xpx}	1
σ^2	$(-1)^{p_4}$	η_σ	1
$\sigma^{-1}C_4\sigma C_4$	$(-1)^{p_7}$	$\eta_{\sigma C_4}$	1
C_4^4	1	η_{C_4}	-1
$C_4^{-1}T_1C_4T_2$	1	-1	-1
$C_4^{-1}T_2C_4T_1^{-1}$	$(-1)^{p_2+p_3}$	$-\eta_{xpx}\eta_{xpy}$	1
$C_4^{-1}\mathcal{T}^{-1}C_4\mathcal{T}$	$(-1)^{p_7}$	$\eta_{C_4\mathcal{T}}$	1
$\sigma^{-1}\mathcal{T}^{-1}\sigma\mathcal{T}$	$(-1)^{p_4}$	$\eta_{\sigma\mathcal{T}}$	1
$T_1^{-1}\mathcal{T}^{-1}T_1\mathcal{T}$	$(-1)^{p_8}$	η_t	1
$T_2^{-1}\mathcal{T}^{-1}T_2\mathcal{T}$	$(-1)^{p_8}$	η_t	1
\mathcal{T}^2	-1	-1	1

TABLE II: Correspondence between bosonic and fermionic PSGs. The bosonic PSGs are labeled by six integers $p_i = 0, 1$ ($i = 1, 2, 3, 4, 7, 8$), while fermionic PSGs are labeled by nine integers ($\eta_{xy}, \eta_{xpy}, \eta_{xpx}, \eta_\sigma, \eta_{C_4}, \eta_{\sigma C_4}, \eta_{C_4\mathcal{T}}, \eta_{\sigma\mathcal{T}}, \eta_t$) where $\eta = \pm 1$. The vison PSG are fully determined as shown in Appendix E. The identity $C_4^{-1}T_1C_4T_2$ is not gauge invariant as we can always tune the relative phase between the gauge transformation G_{T_1} and G_{T_2} , therefore its PSGs can always be fixed as shown above. The vison PSGs can be obtained from the product of fermionic PSGs and bosonic PSGs except the two cases C_4^4 and σ^2 where an extra factor of (-1) should be taken into consideration as discussed in the main text.

The Abrikosov fermion construction of the Heisenberg model and its PSG study is summarized in detail in Wen’s paper²⁷. Although the solutions of the fermionic PSG are under certain gauge, the universal data is encoded in the fractionalization classes as in the case of Schwinger boson, and therefore we obtain the fractionalization classes of the Abrikosov fermion as listed in TABLE II.

In the mean-field level, visons can be considered as point-like excitation located on the center of a plaque-

tte. Due to the Z_2 nature, two visons will annihilate each other, therefore we shall use v to denote vison creation or annihilation operator. The dynamics of the vison can thus be described by a Ising gauge theory^{40–44} and its symmetry fractionalization can be totally determined^{43,44}. The vison PSGs are determined as listed in TABLE II. The detailed calculation is summarized in Appendix E.

In most cases, the twist factor from the mutual statistics of bosons and visons is trivial, but there are three exceptions where the twist factor are nontrivial ($e^{i\phi_t} = -1$), discussed in Ref. 33,34,39. In the following we sketch their arguments for these nontrivial twist phase factors.

The first nontrivial case is C_4^4 , namely fourfold rotation acted by four times^{33,34}. Consider the bound state of a vison and a bosonic spinon, which fuse into a fermionic spinon. When the bound state is rotated around a loop under the operation of C_4^4 , the vison will encycle the boson once and therefore pick up a Berry phase of π ^{33,34,43}.

The second case is σ^2 , namely mirror reflection acted by two times, as discussed by Lu *et al.*³⁴ and Qi *et al.*³⁹. Consider a system consisting of two fermions f_1 and f_2 that can be related by a mirror reflection σ . Then we have $\sigma f_1 \sigma^{-1} = e^{i\phi_1} f_2$, $\sigma f_2 \sigma^{-1} = e^{i\phi_2} f_1$. Therefore acting σ twice on f_1 will yield a factor of $e^{i\phi_f} = e^{i\phi_1} \cdot e^{i\phi_2}$. Alternatively, acting σ once on the pair f_1 and f_2 will yield a factor of $-e^{i\phi_1} \cdot e^{i\phi_2}$, in which the minus sign originates from the exchange the two fermions under σ .

The same argument works for the boson pair and vison pair, but since there is no additional statistical sign as in the case of fermion, we notice that the extra phase factor after acting σ twice on the bosonic spinon or vison is the same as the phase factor after acting σ once on a pair of bosonic spinons or visons. If we denote the phase acquired by acting σ twice on $b(v)$ as $e^{i\phi_b}(e^{i\phi_v})$, then the above statement is equivalent to $-e^{i\phi_1} \cdot e^{i\phi_2} = e^{i\phi_b} \cdot e^{i\phi_v}$ (since we can simply treat f as the bound state of b and v).

Therefore we have the nontrivial fusion rule for the PSG of σ^2 : $e^{i\phi_f} = -e^{i\phi_b} \cdot e^{i\phi_v}$.

The third nontrivial fusion rule comes from $\sigma^{-1}\mathcal{T}\sigma\mathcal{T}$.

Let's consider a system composed of a pair of fermionic spinons f_1 and f_2 located on the X-axis, so that they are symmetric under reflection σ . And we adopt another assumption that the two fermions can be connected by translation T_x , which ensures the two fermions share the same symmetry quantum numbers.

In this case, the system is an eigenstate of the operator σ , we therefore have $\sigma f_1 \sigma^{-1} = e^{i\phi_1} f_1$, $\sigma f_2 \sigma^{-1} = e^{i\phi_1} f_2$. And acting σ twice on a fermion will yield a factor of $e^{i\phi_f} = e^{2i\phi_1}$.

Consider a pair of bosonic spinons and visons located on the X-axis, and we denote the eigenvalue of $b(v)$ under σ as $e^{i\phi_2}(e^{i\phi_3})$. Acting σ twice on a boson(vison) will yield a factor of $e^{i\phi_b} = e^{2i\phi_2}(e^{2i\phi_3})$.

If we treat the fermion as the bound state of a boson and a vison, then from the above discussion we have $e^{2i\phi_1} = -e^{2i\phi_2} \cdot e^{2i\phi_3}$. By splitting -1 equally into the

two fermion sectors, we have $e^{i\phi_1} = (\pm i)e^{i\phi_2} \cdot e^{i\phi_3}$, which means each fermionic spinon gets an extra $\pm i$ phase in addition to the phase acquired by the boson and vison under reflection σ . But since the time-reversal transformation will take a number to its complex conjugate, the extra phase will be $(\pm i)^*(\pm i) = 1$ under the symmetry operation $(\sigma\mathcal{T})^2$, which indicates that $(\sigma\mathcal{T})^2$ has a trivial fusion rule.

Consider the following algebraic identity

$$(\mathcal{T}\sigma)^2 = (\sigma^{-1}\mathcal{T}^{-1}\sigma\mathcal{T}) \cdot (\mathcal{T})^2 \cdot (\sigma)^2, \quad (55)$$

since the fusion rule for $(\mathcal{T}\sigma)^2$ and \mathcal{T}^2 are both trivial, while the fusion rule for σ^2 is nontrivial, we know that the fusion rule for $\sigma^{-1}\mathcal{T}^{-1}\sigma\mathcal{T}$ is nontrivial.

Notice that the fourfold rotational symmetry C_4 is a combination of two reflection symmetry $C_4 = P_{xy}\sigma$, where P_{xy} is defined as the reflection along $y = x$. Therefore from the algebraic identity

$$C_4^{-1}\mathcal{T}^{-1}C_4\mathcal{T} = (P_{xy}^{-1}\mathcal{T}^{-1}P_{xy}\mathcal{T}) \cdot (\sigma^{-1}\mathcal{T}^{-1}\sigma\mathcal{T}), \quad (56)$$

we know that the fusion rule for $C_4^{-1}\mathcal{T}^{-1}C_4\mathcal{T}$ is trivial.

The correspondence of fermionic PSGs and bosonic PSGs are listed in TABLE II. From the fusion rule, we find Z_2 spin liquids that can be both described by fermionic and bosonic partons if the following conditions are satisfied:

$$\begin{aligned} \eta_{xy} &= (-1)^{p_1+1}, \quad \eta_{xpx} = (-1)^{p_3}, \quad \eta_{xpy} = (-1)^{p_2+1}, \\ \eta_t &= (-1)^{p_8}, \quad \eta_{\sigma\mathcal{T}} = \eta_{\sigma} = (-1)^{p_4+1}, \quad \eta_{\sigma C_4} = \eta_{C_4\mathcal{T}} = (-1)^{p_7}, \\ \eta_{C_4} &= 1, \end{aligned} \quad (57)$$

where the η s are ± 1 which label different fractionalization classes of fermionic spinons (see Appendix F for their definitions).

All the six Schwinger boson Z_2 spin liquid states we have discussed have fermionic counterparts. The Schwinger boson $Z_2[0,0]$ state has two fermionic counterparts, which are $Z_2 B\tau_-^1\tau_-^1\tau_-^1\tau_-^3$ state and $Z_2 B\tau_-^2\tau_-^2\tau_-^1\tau_-^3$ state. The Schwinger boson $Z_2[0,\pi]$ state, $Z_2[\pi,0]\mathcal{R}$ state and $Z_2[\pi,0]\mathcal{I}$ state correspond to $Z_2 B\tau_-^1\tau_-^1\tau_-^0\tau_-^3$ state, $Z_2 A\tau_-^1\tau_-^1\tau_-^0\tau_-^3$ state and $Z_2 A\tau_-^1\tau_-^1\tau_-^0\tau_-^3$ state respectively. The Schwinger boson $Z_2[\pi,\pi]\mathcal{R}$ state corresponds to $Z_2 A\tau_+^0\tau_+^0\tau_+^0\tau_+^0$ and $Z_2 A\tau_+^0\tau_+^0\tau_+^0\tau_+^3$ state. The Schwinger boson $Z_2[\pi,\pi]\mathcal{I}$ state corresponds to $Z_2 A\tau_+^0\tau_+^0\tau_+^0\tau_+^0$ and $Z_2 A\tau_+^0\tau_+^0\tau_+^0\tau_+^3$ state. See TABLE III. Their possible realization on square lattice is discussed in Appendix G. Among these nine states, the $Z_2 A\tau_+^0\tau_+^0\tau_+^0\tau_+^0$ state cannot be realized by mean-field ansatz, and the $Z_2 A\tau_+^0\tau_+^0\tau_+^0\tau_+^0$ state is a gapless spin liquid state whose gaplessness is protected by its PSG⁵¹, and the remaining PSGs can all be realized by gapped spin liquid states.

IV. DISCUSSIONS AND SUMMARY

Here we discuss the relation between our results and related theoretical and experimental works. The PSG classification of Schwinger boson states has been used in Tao

Schwinger boson		Abrikosov fermion						
$(p_1, p_2, p_3, p_4, p_7, p_8)$	Label	$(\eta_{xy}, \eta_{xpx}, \eta_{xpy}, \eta_t)$	g_{P_x}	g_{P_y}	$g_{P_{xy}}$	$g_{\mathcal{T}}$	Label	Perturbatively gapped?
(0,0,1,0,0,1)	$Z_2[0, 0]$	(-1,-1,-1,-1)	$i\tau^1$	$i\tau^1$	$i\tau^1$	$i\tau^3$	$Z_2B\tau_-^1\tau_-^1\tau_-^1\tau_-^3$	Yes
			$i\tau^2$	$i\tau^2$	$i\tau^1$	$i\tau^3$	$Z_2B\tau_-^2\tau_-^2\tau_-^1\tau_-^3$	Yes
(0,0,1,0,1,1)	$Z_2[0, \pi]$	(-1,-1,-1,-1)	$i\tau^1$	$i\tau^1$	τ^0	$i\tau^3$	$Z_2B\tau_-^1\tau_-^1\tau_-^0\tau_-^3$	Yes
(1,0,1,0,1,0)	$Z_2[\pi, 0]\mathcal{R}$	(1,-1,-1,1)	$i\tau^1$	$i\tau^1$	τ^0	$i\tau^3$	$Z_2A\tau_+^1\tau_+^1\tau_+^0\tau_+^3$	Yes
(1,0,1,0,1,1)	$Z_2[\pi, 0]\mathcal{I}$	(1,-1,-1,-1)	$i\tau^1$	$i\tau^1$	τ^0	$i\tau^3$	$Z_2A\tau_+^1\tau_+^1\tau_+^0\tau_+^3$	Yes
(1,1,0,1,0,0)	$Z_2[\pi, \pi]\mathcal{R}$	(1,1,1,1)	τ^0	τ^0	τ^0	τ^0	$Z_2A\tau_+^0\tau_+^0\tau_+^0\tau_+^0$	—
			τ^0	τ^0	τ^0	$i\tau^3$	$Z_2A\tau_+^0\tau_+^0\tau_+^0\tau_+^3$	Yes
(1,1,0,1,0,1)	$Z_2[\pi, \pi]\mathcal{I}$	(1,1,1,-1)	τ^0	τ^0	τ^0	τ^0	$Z_2A\tau_+^0\tau_+^0\tau_+^0\tau_+^0$	No
			τ^0	τ^0	τ^0	$i\tau^3$	$Z_2A\tau_+^0\tau_+^0\tau_+^0\tau_+^3$	Yes

TABLE III: Correspondence between PSG solutions of bosonic and fermionic Z_2 spin liquids. The Schwinger boson $Z_2[0, 0]$ state has two fermionic counterparts, which are $Z_2B\tau_-^1\tau_-^1\tau_-^1\tau_-^3$ state and $Z_2B\tau_-^2\tau_-^2\tau_-^1\tau_-^3$ state. The Schwinger boson $Z_2[0, \pi]$ state, $Z_2[\pi, 0]\mathcal{R}$ state and $Z_2[\pi, 0]\mathcal{I}$ state correspond to $Z_2B\tau_-^1\tau_-^1\tau_-^0\tau_-^3$ state, $Z_2A\tau_+^1\tau_+^1\tau_+^0\tau_+^3$ state and $Z_2A\tau_+^1\tau_+^1\tau_+^0\tau_+^3$ state respectively. The Schwinger boson $Z_2[\pi, \pi]\mathcal{R}$ state corresponds to $Z_2A\tau_+^0\tau_+^0\tau_+^0\tau_+^0$ and $Z_2A\tau_+^0\tau_+^0\tau_+^0\tau_+^3$ state, of which the $Z_2A\tau_+^0\tau_+^0\tau_+^0\tau_+^0$ state does not have a mean-field realization²⁷. The Schwinger boson $Z_2[\pi, \pi]\mathcal{I}$ state corresponds to $Z_2A\tau_+^0\tau_+^0\tau_+^0\tau_+^0$ and $Z_2A\tau_+^0\tau_+^0\tau_+^0\tau_+^3$ state. Among the eight PSGs that have mean-field realization, only the $Z_2A\tau_+^0\tau_+^0\tau_+^0\tau_+^0$ is a gapless state whose gaplessness is protected by its PSG⁵¹. The remaining seven PSGs can all be realized by gapped spin liquid states.

Li *et al*⁴⁹ and Yi-Zhuang You *et al*¹¹. In particular Tao Li and coworkers studied the energetics of several kinds of projected Schwinger boson wave functions on square lattice for J_1 - J_2 Heisenberg model⁴⁹. However they did not provide a complete projective symmetry group analysis and presented numerical results for zero-flux states only. Yi-Zhuang You and coworkers tried to explain the behavior of local moments in iron-based superconductors by Schwinger boson spin liquid states⁷. They achieved a complete solution of algebraic PSG in appendix, but did not study all the mean-field states. As far as we know our paper is the first complete account on the PSG classification and mean-field realizations of Schwinger boson spin liquid states on square lattice, as well as the magnetic orders connected to Schwinger boson Z_2 spin liquids.

We do not attempt to relate our results directly to any experimental or numerical evidences of spin liquids. It may be tempting to try to relate these Z_2 spin liquids with underdoped cuprate superconductors. This possibility has been thoroughly discussed in the review by Lee and coworkers⁵, albeit using a different slave-particle formalism with fermionic spinons. If the relation between Schwinger boson and Abrikosov fermion spin liquids can be firmly established, our results may also be relevant to cuprates. More recently an inelastic neutron scattering experiment observed evidence of spinons coexisting with Néel order⁵⁰. This type of states is beyond our current study of *symmetric* spin liquids without any symmetry breaking. Classification and numerical studies of this type of “AFM*” states will be an interesting future direction.

Finally we would like to say a few more words about the relation between Schwinger boson and Abrikosov fermion spin liquid states.

Several groups^{39,46-48} have established the exact mapping between these two formulations on extremely short-range(nearest-neighbor) resonating valence bond(RVB)

states, which are limiting cases of Gutzwiller projected wave functions of mean-field Schwinger boson or Abrikosov fermion states. This exact mapping however is not very useful on square lattice. There are two nearest-neighbor RVB states on square lattice preserving all lattice symmetry. They correspond to the zero-flux Schwinger boson(π -flux Abrikosov fermion) states and the π -flux Schwinger boson(zero-flux Abrikosov fermion) states respectively. However the nearest-neighbor RVB states on square lattice are not Z_2 spin liquids²⁷, and they cannot distinguish different mean-field ansatz with the same flux in elementary plaquette. To represent Z_2 spin liquids and distinguish all PSG classes, valence bonds beyond nearest-neighbors will be required. We have checked on small lattices that the exact mapping for the nearest-neighbor RVB states^{39,46-48} cannot be established with long range valence bonds.

In summary, we have studied Schwinger boson spin liquid states on square lattice by the projective symmetry group analysis and Schwinger boson mean-field theory. Six symmetric Z_2 spin liquid states, two zero-flux states and four π -flux states, have been identified to be possibly relevant to the J_1 - J_2 model. The zero-flux states can go through continuous phase transitions into canted or collinear Néel order. However these magnetic orders always show nonzero vector spin chirality $\langle \mathbf{S}_i \times \mathbf{S}_j \rangle$, even if the spin expectation values are collinear. The π -flux states are in proximity to certain 4-sublattice magnetic orders including the Néel order, and can be favored energetically over zero-flux states with ring-exchange interactions²⁸. At mean-field level, two of the π -flux states, the $Z_2[\pi, \pi]\mathcal{R}$ and $Z_2[\pi, \pi]\mathcal{I}$ states, may be stable against magnetic order for spin-1/2 and around $J_2/J_1 \sim 1/2$. We have computed the bottom of two-spinon excitation continuum and static spin structure factors for these spin liquid states, which can be used in numerics and experiments as indirect evidences

of these spin liquids. Our results can be used in further theoretical studies of spin liquids on square lattice, for example in variational Monte Carlo calculations of projected bosonic spin liquid wave functions.

Acknowledgments

The authors thank Ashvin Vishwanath and Yuan-Ming Lu for helpful discussions, and thank Shubhayu Chatterjee and Yuan-Ming Lu for pointing out two mistakes in previous version of this paper. FW acknowledges support from National Key Basic Research Program of China (Grant No. 2014CB920902) and National Natural Science Foundation of China (Grant No. 11374018).

Appendix A: Solution of the algebraic PSG

In the following we will solve the algebraic PSGs by using the algebraic constraints on the generators of the square lattice space group.

For reasons discussed in the introduction, the low energy gauge group after Higgs condensation is Z_2 , which is called the invariant gauge group (IGG) of the PSG.

The two elements of the IGG are identity operator and the generator

$$b_{j\alpha} \rightarrow -b_{j\alpha}. \quad (\text{A1})$$

For future convenience, we introduce two difference operators Δ_x and Δ_y defined as $\Delta_x f(x, y) = f(x, y) - f(x-1, y)$ and $\Delta_y f(x, y) = f(x, y) - f(x, y-1)$.

The PSG is solved under certain gauge, therefore it is important to consider how PSG elements change if we do a gauge transformation to the ansatz.

When a gauge transformation $G : b_{j\alpha} \rightarrow e^{i\phi(j)} b_{j\alpha}$ is applied to the ansatz, the ansatz will be invariant under $GG_X XG^{-1} = GG_X XG^{-1} X^{-1} X$, therefore G_X is now converted to $GG_X XG^{-1} X^{-1}$ and the phase functions changes according to:

$$\phi_X(\mathbf{r}) \rightarrow \phi_G(\mathbf{r}) + \phi_X(\mathbf{r}) - \phi_G[X^{-1}(\mathbf{r})]. \quad (\text{A2})$$

With this recipe we can use the gauge freedom to do the gauge fixing procedure on a spanning tree (an open boundary condition is assumed), thus the gauge is fixed to be

$$\phi_{T_1}(x, y) = 0, \quad \phi_{T_2}(0, y) = 0. \quad (\text{A3})$$

The commutative relation $T_1^{-1} T_2 T_1 T_2^{-1} = \mathbf{1}$, when translated into the PSG language, is

$$T_1^{-1} G_{T_1}^{-1} G_{T_2} T_2 G_{T_1} T_1 T_2^{-1} G_{T_2}^{-1} \in IGG, \quad (\text{A4})$$

therefore $\Delta_x \phi_{T_2}(x, y) = p_1 \pi$ (in this and next section, all the equations are true modulo 2π). Here the number p_1 is either 0 or 1 due to the Z_2 gauge structure. Integers $p_i, i = 2, 3, \dots, 9$ appeared later are also Z_2 integers.

After gauge fixing procedure, we are still left with three gauge freedom which will not change ϕ_{T_1}, ϕ_{T_2} up to IGG elements but may affect other PSG elements.

$$G_1 : \phi_1(x, y) = \text{const.}, \quad (\text{A5})$$

$$G_2 : \phi_2(x, y) = \pi x, \quad (\text{A6})$$

$$G_3 : \phi_3(x, y) = \pi y. \quad (\text{A7})$$

We are left with commutative relations, $\sigma^{-1} T_1 \sigma T_1^{-1} = \sigma^{-1} T_2 \sigma T_2^{-1} = \sigma^2 = \sigma^{-1} C_4 \sigma C_4 = C_4^4 = C_4^{-1} T_1 C_4 T_2 = \mathbf{1}$, and four commutative relations concerning time reversal symmetry, $\mathcal{T}^{-1} T_1 \mathcal{T} T_1^{-1} = \mathcal{T}^{-1} T_2 \mathcal{T} T_2^{-1} = \mathcal{T}^{-1} \sigma \mathcal{T} \sigma^{-1} = \mathcal{T}^{-1} C_4 \mathcal{T} C_4^{-1} = \mathbf{1}$.

Using the condition $\sigma^{-1} T_1 \sigma T_1^{-1} = \mathbf{1}$, and $\sigma^{-1} T_2 \sigma T_2^{-1} = \mathbf{1}$, we can obtain:

$$\Delta_x \phi_\sigma(x, y) = p_2 \pi, \quad (\text{A8})$$

$$\Delta_y \phi_\sigma(x, y) = p_3 \pi, \quad (\text{A9})$$

whose solution is $\phi_\sigma(x, y) = p_2 \pi x + p_3 \pi y + \phi_\sigma(0, 0)$.

The constraint from $\sigma^2 = \mathbf{1}$ is $2\phi_\sigma(0, 0) = p_4 \pi$. Due the Z_2 gauge structure, an overall phase π has no consequence and hence we can fix $\phi_\sigma(0, 0)$ to be $p_4 \pi / 2$.

Therefore we have

$$\phi_\sigma(x, y) = p_2 \pi x + p_3 \pi y + p_4 \pi / 2. \quad (\text{A10})$$

The gauge condition G_1, G_2 and G_3 have no effect on it.

Consider the fourfold rotation C_4 .

From $C_4^{-1} T_1 C_4 T_2 = \mathbf{1}$ and $C_4^{-1} T_2 C_4 T_1^{-1} = \mathbf{1}$ we have

$$\Delta_x \phi_{C_4} = p_1 \pi y + p_5 \pi, \quad (\text{A11})$$

$$\Delta_y \phi_{C_4} = p_1 \pi x + p_6 \pi, \quad (\text{A12})$$

the solution of which is $\phi_{C_4}(x, y) = p_1 \pi xy + p_5 \pi x + p_6 \pi y + \phi_{C_4}(0, 0)$.

From $C_4 \sigma C_4 \sigma^{-1} = \mathbf{1}$ we have

$$p_2 + p_3 + p_5 + p_6 = 0, \quad 2\phi_{C_4} = p_7 \pi. \quad (\text{A13})$$

The gauge condition G_2 can tune p_5 to be zero. And the condition $C_4^4 = \mathbf{1}$ gives no new constraint.

Therefore we have

$$\phi_{C_4}(x, y) = p_1 \pi xy + p_6 \pi y + p_7 \pi / 2. \quad (\text{A14})$$

As for time-reversal symmetry, the condition $\mathcal{T}^{-1} T_1 \mathcal{T} T_1^{-1} = \mathbf{1}$ and $\mathcal{T}^{-1} T_2 \mathcal{T} T_2^{-1} = \mathbf{1}$ yield

$$\Delta_x \phi_{\mathcal{T}} = p_8 \pi, \quad (\text{A15})$$

$$\Delta_y \phi_{\mathcal{T}} = p_9 \pi. \quad (\text{A16})$$

Therefore we have

$$\phi_{\mathcal{T}}(x, y) = p_8 \pi x + p_9 \pi y + \phi_{\mathcal{T}}(0, 0) \quad (\text{A17})$$

The condition $\mathcal{T}^{-1} \sigma \mathcal{T} \sigma^{-1} = \mathbf{1}$ produces no constraint. The condition $\mathcal{T}^{-1} C_4 \mathcal{T} C_4^{-1} = \mathbf{1}$ requires that $p_8 = p_9$.

Note that the gauge condition $G_1(b_{j\alpha}) = e^{i\phi_1} b_{j\alpha}$ acts nontrivially in respect of the time reversal symmetry since time reversal operator will change a number to its complex conjugate. After gauge transformation G_1 , the phase function changes as

$$\phi_{\mathcal{T}}(\mathbf{r}) \rightarrow \phi_{\mathcal{T}}(\mathbf{r}) + 2\phi_1 \quad (\text{A18})$$

Therefore we may use the gauge condition G_1 to fix $\phi_{\mathcal{T}}(0, 0)$ to be $-p_8\pi/2$, so we finally obtain

$$\phi_{\mathcal{T}}(\mathbf{r}) = p_8(x + y - 1/2)\pi. \quad (\text{A19})$$

Finally the algebraic solutions of PSG are:

$$\phi_{T_1} = 0, \quad (\text{A20})$$

$$\phi_{T_2} = p_1\pi x, \quad (\text{A21})$$

$$\phi_{\sigma} = p_2\pi x + p_3\pi y + \frac{p_4\pi}{2}, \quad (\text{A22})$$

$$\phi_{C_4} = p_1\pi xy + (p_2 + p_3)\pi y + \frac{p_7\pi}{2}, \quad (\text{A23})$$

$$\phi_{\mathcal{T}} = p_8(x + y - 1/2)\pi. \quad (\text{A24})$$

There are two choices for each p_i ($i = 1, 2, 3, 4, 7, 8$), so total amounts of PSG solutions are $2^6 = 64$.

Appendix B: Physical realizations of PSG on square lattice

PSG solved by the commutative relations of group generators is called the algebraic PSG since it relies only on the structure of the symmetry group and may not be realized by a mean-field ansatz.

Generally speaking, realization of a particular kind of ansatz on square lattice will impose further constraints on algebraic PSG, therefore it is necessary to analyze the constraints imposed on PSG when demanding that an arbitrary bond u_{ij} (u_{ij} represents A_{ij} or B_{ij}) is nonvanishing.

We shall only consider bonds that start from the original point $(x, y) = (0, 0)$ since other bonds can be obtained by translation.

1. $u_{(0,0)\rightarrow(x,x)}$

The bond $A_{(0,0)\rightarrow(x,x)}$ becomes $A_{(x,x)\rightarrow(0,0)}$ under symmetry operation $T_2^x T_1^x C_4^2$. Since A_{ij} is antisymmetric, *i.e.* $A_{ij} = -A_{ji}$, we have:

$$[G_{T_2} T_2]^x [G_{T_1} T_1]^x [G_{C_4} C_4]^2 A_{(0,0)\rightarrow(x,x)} = -A_{(0,0)\rightarrow(x,x)}, \quad (\text{B1})$$

thus we have

$$2\phi_{C_4}(0, 0) + \phi_{C_4}(-x, x) + \phi_{C_4}(-x, -x) + \sum_{i=1}^x (\phi_{T_2}(0, -x+i) + \phi_{T_2}(x, i)) = \pi, \quad (\text{B2})$$

therefore $p_1\pi x^2 = \pi$.

$A_{(0,0)\rightarrow(x,x)}$ is invariant under the combined operation $C_4\sigma$, so we have:

$$\begin{aligned} & \phi_{C_4}(0, 0) + \phi_{C_4}(x, x) + \phi_{\sigma}(0, 0) + \phi_{\sigma}(x, -x) \\ & = p_1\pi x + (p_4 + p_7)\pi = 0. \end{aligned} \quad (\text{B3})$$

Therefore when x is odd, the condition (B2) and (B3) are satisfied only when $p_1 = p_4 + p_7 = 1$, and when x is even, the two conditions cannot be satisfied simultaneously and hence $A_{(0,0)\rightarrow(x,x)}$ vanishes.

$B_{(0,0)\rightarrow(x,x)}$ becomes $B_{(0,0)\rightarrow(x,x)}^*$ under $T_2^x T_1^x C_4^2$, so we have

$$\begin{aligned} & \phi_{C_4}(-x, x) + \phi_{C_4}(-x, -x) - 2\phi_{C_4}(0, 0) \\ & + \sum_{i=1}^x (\phi_{T_2}(0, -x+i) - \phi_{T_2}(x, i)) \\ & = p_1\pi x^2 = \text{Arg}(B_{(0,0)\rightarrow(x,x)}^*/B_{(0,0)\rightarrow(x,x)}). \end{aligned} \quad (\text{B4})$$

$B_{(0,0)\rightarrow(x,x)}$ is invariant under $C_4\sigma$, so we have

$$-\phi_{C_4}(0, 0) + \phi_{C_4}(x, x) - \phi_{\sigma}(0, 0) + \phi_{\sigma}(x, -x) = p_1\pi x^2 = 0. \quad (\text{B5})$$

When x is even, the condition (B4) and (B5) demand that $B_{(0,0)\rightarrow(x,x)}$ is real. When x is odd, (B5) demands that $p_1 = 1$ and (B4) demands that $B_{(0,0)\rightarrow(x,x)}$ is real.

The results are summarized in Table IV.

$A_{(0,0)\rightarrow(x,x)}$	$B_{(0,0)\rightarrow(x,x)}$	$x \pmod{2}$
vanish	$\text{Im}(B)=0$	0
$p_1 = p_4 + p_7 = 1$	$p_1 = 0, \text{Im}(B)=0$	1

TABLE IV: Constraint imposed on PSG by nonvanishing bond $u_{(0,0)\rightarrow(x,x)}$

2. $u_{(0,0)\rightarrow(x,0)}$

The bond $A_{(0,0)\rightarrow(x,0)}$ is invariant under σ , so

$$\phi_{\sigma}(0, 0) + \phi_{\sigma}(x, 0) = p_2\pi x + p_4\pi = 0. \quad (\text{B6})$$

This bond becomes its inverse under $T_1^x C_4^2$, thus we have

$$\begin{aligned} & 2\phi_{C_4}(0, 0) + \phi_{C_4}(0, x) + \phi_{C_4}(-x, 0) \\ & = (p_2 + p_3)\pi x = \pi. \end{aligned} \quad (\text{B7})$$

When x is even, the condition (B7) cannot be satisfied. When x is odd, the condition (B6) demands that $p_2 + p_4 = 0$ and the condition (B7) demands that $p_2 + p_3 = 1$.

$B_{(0,0)\rightarrow(x,0)}$ is invariant under σ , so

$$-\phi_{\sigma}(0, 0) + \phi_{\sigma}(x, 0) = p_2\pi x = 0. \quad (\text{B8})$$

This bond becomes its conjugate under $T_1^x C_4^2$, therefore we have

$$\begin{aligned} & -2\phi_{C_4}(0, 0) + \phi_{C_4}(0, x) + \phi_{C_4}(-x, 0) \\ & = \text{Arg}(B_{(0,0)\rightarrow(x,0)}^*/B_{(0,0)\rightarrow(x,0)}). \end{aligned} \quad (\text{B9})$$

When x is even, we have $\text{Arg}(B^*/B)=0$. When x is odd, we know from (B8) that $p_2 = 0$. And the condition (B9) demands that $\text{Arg}(B^*/B)=p_3\pi$.

The results are summarized in Table V.

$A_{(0,0)\rightarrow(x,0)}$	$B_{(0,0)\rightarrow(x,0)}$	$x \pmod{2}$
vanish	$\text{Im}(B)=0$	0
$p_2 + p_3 = 1, p_4 = p_2$	$p_2 = p_3 = 0, \text{Im}(B)=0$ or $p_2 = 0, p_3 = 1, \text{Re}(B)=0$	1

TABLE V: Constraint imposed on PSG by nonvanishing bond $u_{(0,0)\rightarrow(x,0)}$

3. $u_{(0,0)\rightarrow(x,y)}, x \neq y$

There is only one constraint:

$$[G_{T_2}T_2]^y[G_{T_1}T_1]^x[G_{C_4}C_4]^2A_{(0,0)\rightarrow(x,y)} = -A_{(0,0)\rightarrow(x,y)},$$

which leads to

$$\begin{aligned} & 2\phi_{C_4}(0,0) + \phi_{C_4}(-y,x) + \phi_{C_4}(-x,-y) \\ & + \sum_{i=1}^y (\phi_{T_2}(0,-y+i) + \phi_{T_2}(x,i)) \\ & = p_1\pi xy + (p_2 + p_3)\pi(x-y) = \pi. \end{aligned} \quad (\text{B10})$$

When x and y are both even, the condition (B10) cannot be satisfied, therefore $A_{(0,0)\rightarrow(x,y)}$ vanishes. When $x + y$ is odd, the condition (B10) is satisfied when $p_2 + p_3 = 1$. When x and y are both odd, the condition (B10) demands that $p_1 = 1$.

As for $B_{(0,0)\rightarrow(x,y)}$, we have

$$\begin{aligned} & -2\phi_{C_4}(0,0) + \phi_{C_4}(-y,x) + \phi_{C_4}(-x,-y) \\ & + \sum_{i=1}^y (\phi_{T_2}(0,-y+i) - \phi_{T_2}(x,i)) \\ & = p_1\pi xy + (p_2 + p_3)\pi(x-y) \\ & = \text{Arg}(B_{(0,0)\rightarrow(x,y)}^*/B_{(0,0)\rightarrow(x,y)}). \end{aligned} \quad (\text{B11})$$

When x and y are both even, the condition (B10) demands that $B_{(0,0)\rightarrow(x,y)}$ is real. When $x + y$ is odd, the condition B10 demands that $\text{Arg}(B^*/B)=(p_2 + p_3)\pi$. When x and y are both odd, the condition (B10) demands that $\text{Arg}(B^*/B)=p_1\pi$.

The results are summarized in Table VI.

Appendix C: Derivation of the magnetic order from the condensation of Schwinger boson in mean-field level

1. Canted Néel order from $Z_2[0,0]$ state

For $Z_2[0,0]$ state, the spinon condensation happens at $\pm\mathbf{Q}$, $\mathbf{Q} = (\pi/2, -\pi/2)$ when $\mu = 2B_2 - 2\sqrt{A_1^2 + B_1^2}$.

$A_{(0,0)\rightarrow(x,y)}$	$B_{(0,0)\rightarrow(x,y)}$	$x \pmod{2}$	$y \pmod{2}$
vanish	$\text{Im}(B)=0$	0	0
$p_2 + p_3 = 1$	$p_2 + p_3 = 0, \text{Im}(B)=0$ or $p_2 + p_3 = 1, \text{Re}(B)=0$	0	1
		1	0
$p_1 = 1$	$p_1 = 0, \text{Im}(B)=0$ or $p_1 = 1, \text{Re}(B)=0$	1	1

TABLE VI: Constraint imposed on PSG by nonvanishing bond $u_{(0,0)\rightarrow(x,y)}$

The zero energy eigenvector of the mean-field Hamiltonian (22) at $\mathbf{Q} = (\pi/2, -\pi/2)$ point is

$$\Psi_1 = \begin{pmatrix} \frac{-iA_1}{\sqrt{B_1^2 + A_1^2} - B_1} \\ 1 \end{pmatrix}. \quad (\text{C1})$$

When boson condense, a ground state expectation value at \mathbf{Q} is obtained: $\langle \Psi(\mathbf{Q}) \rangle = z\Psi_1$.

The zero energy eigenvector at $-\mathbf{Q}$ point is

$$\Psi_2 = \begin{pmatrix} 1 \\ \frac{-iA_1}{\sqrt{B_1^2 + A_1^2} - B_1} \end{pmatrix}. \quad (\text{C2})$$

And the condensation value is $\langle \Psi(-\mathbf{Q}) \rangle = \omega\Psi_2$.

Therefore we can represent the condensation on lattice site \mathbf{r} as:

$$x = \begin{pmatrix} \langle b_{\mathbf{r}\uparrow} \rangle \\ \langle b_{\mathbf{r}\downarrow} \rangle \end{pmatrix} = \begin{pmatrix} z & w \\ -w^* & z^* \end{pmatrix} \begin{pmatrix} \frac{-iA_1}{\sqrt{B_1^2 + A_1^2} - B_1} e^{i\mathbf{Q}\cdot\mathbf{r}} \\ e^{-i\mathbf{Q}\cdot\mathbf{r}} \end{pmatrix}. \quad (\text{C3})$$

The 2×2 matrix is proportional to a $\text{SU}(2)$ matrix and its effect on the order parameter $\langle \mathbf{S}(\mathbf{r}) \rangle$ is just a $\text{SO}(3)$ rotation.

The magnetic order obtained from the spinor x therefore can be computed using

$$\begin{aligned} \langle \mathbf{S}(\mathbf{r}) \rangle &= (1/2)x^\dagger \sigma x \\ &= \frac{1 + (-)^{x+y}}{2} \vec{n}_u + \frac{1 - (-)^{x+y}}{2} \vec{n}_v, \end{aligned} \quad (\text{C4})$$

If we introduce the notion $s = \frac{-iA_1}{\sqrt{B_1^2 + A_1^2} - B_1}$, the vector n_u and n_v can be conveniently represented as

$$\vec{n}_u = (0, 2is, -1 - s^2), \quad (\text{C5})$$

$$\vec{n}_v = (0, -2is, -1 - s^2). \quad (\text{C6})$$

And when $s \neq 0$, we have $\vec{n}_u \cdot \vec{n}_v / (|\vec{n}_u| \cdot |\vec{n}_v|) = \frac{2(|s|^2 - 1)^2}{(|s|^2 + 1)^2} - 1 > -1$. Therefore the magnetic order obtained from the $Z_2[0,0]$ spin liquid is a non-collinear order.

2. Néel order from $Z_2[0,\pi]$ state

For $Z_2[0,\pi]$ state, the spinon condensation happens at $\pm\mathbf{Q}$, $\mathbf{Q} = (\pi/2, \pi/2)$ when $\mu = -2A_1 - 2B_2$.

The zero energy eigenvector at the $\mathbf{Q} = (\pi/2, \pi/2)$ point is

$$\Psi_1 = \begin{pmatrix} 1 \\ i \end{pmatrix}. \quad (\text{C7})$$

When boson condense, the condensation value at \mathbf{Q} is $\langle \Psi(\mathbf{Q}) \rangle = z\Psi_1$.

The zero energy eigenvector at $-\mathbf{Q}$ point is

$$\Psi_2 = \begin{pmatrix} 1 \\ -i \end{pmatrix}. \quad (\text{C8})$$

And the condensation value is $\langle \Psi(-\mathbf{Q}) \rangle = \omega\Psi_2$.

Therefore we can represent the condensation on lattice site \mathbf{r} as:

$$x = \begin{pmatrix} \langle b_{\mathbf{r}\uparrow} \rangle \\ \langle b_{\mathbf{r}\downarrow} \rangle \end{pmatrix} = \begin{pmatrix} z & w \\ iw^* & -iz^* \end{pmatrix} \begin{pmatrix} e^{i\mathbf{Q}\cdot\mathbf{r}} \\ e^{-i\mathbf{Q}\cdot\mathbf{r}} \end{pmatrix}, \quad (\text{C9})$$

where the 2×2 matrix is proportional to a SU(2) matrix and its effect on the order parameter $\langle \mathbf{S}(\mathbf{r}) \rangle$ is an SO(3) rotation.

The magnetic order obtained from the spinor x is therefore

$$\begin{aligned} \langle \mathbf{S}(\mathbf{r}) \rangle &= (1/2)x^\dagger \sigma x \\ &= \cos(2\mathbf{Q} \cdot \mathbf{r}) \mathbf{m} = (-)^{x+y} \mathbf{m}, \end{aligned} \quad (\text{C10})$$

which is the Néel order.

3. Magnetic order from π -flux states

For π flux state with only nearest bond A_1 , the spinon condensation occurs at $\pm\mathbf{Q}$, $\mathbf{Q} = (\pi/2, \pi/2)$ when $\mu = -2A_1$.

We divide the system into two sets of sublattice which are distinguished by $(-1)^y$ which are labeled by u and v separately.

At \mathbf{Q} , the Hamiltonian has two linearly independent eigenvectors:

$$\begin{aligned} \Psi_1 &= (1, 0, \frac{i}{\sqrt{2}}, \frac{1}{\sqrt{2}})^T, \\ \Psi_2 &= (0, 1, -\frac{1}{\sqrt{2}}, -\frac{i}{\sqrt{2}})^T. \end{aligned} \quad (\text{C11})$$

The condensate at \mathbf{Q} is the linear combination of the two eigenvectors

$$\langle \Psi(\mathbf{Q}) \rangle = z_1\Psi_1 + z_2\Psi_2. \quad (\text{C12})$$

At $-\mathbf{Q}$ point, the two eigenvectors are:

$$\begin{aligned} \Psi_3 &= (-\frac{i}{\sqrt{2}}, \frac{1}{\sqrt{2}}, -1, 0)^T, \\ \Psi_4 &= (-\frac{1}{\sqrt{2}}, \frac{i}{\sqrt{2}}, 0, -1)^T. \end{aligned} \quad (\text{C13})$$

The condensation at $-\mathbf{Q}$ is the linear combination of Ψ_3 and Ψ_4

$$\langle \Psi(-\mathbf{Q}) \rangle = \omega_1\Psi_3 + \omega_2\Psi_4. \quad (\text{C14})$$

In real space, we have

$$\begin{pmatrix} \langle b_{u\mathbf{r}\uparrow} \rangle \\ \langle b_{v\mathbf{r}\uparrow} \rangle \\ \langle b_{u\mathbf{r}\downarrow} \rangle \\ \langle b_{v\mathbf{r}\downarrow} \rangle \end{pmatrix} = e^{i\mathbf{Q}\cdot\mathbf{r}} [z_1\Psi_1 + z_2\Psi_2] + e^{-i\mathbf{Q}\cdot\mathbf{r}} [\omega_1\Psi_3 + \omega_2\Psi_4]. \quad (\text{C15})$$

Therefore the condensate on lattice \mathbf{r} can be represented as:

$$\begin{aligned} x_u &\equiv \begin{pmatrix} \langle b_{u\mathbf{r}\uparrow} \rangle \\ \langle b_{u\mathbf{r}\downarrow} \rangle \end{pmatrix} \\ &= \begin{pmatrix} z_1 & -\frac{i}{\sqrt{2}}w_1 - \frac{1}{\sqrt{2}}w_2 \\ -w_1^* & \frac{i}{\sqrt{2}}z_1^* - \frac{1}{\sqrt{2}}z_2^* \end{pmatrix} \begin{pmatrix} e^{i\mathbf{Q}\cdot\mathbf{r}} \\ e^{-i\mathbf{Q}\cdot\mathbf{r}} \end{pmatrix}, \end{aligned} \quad (\text{C16})$$

$$\begin{aligned} x_v &\equiv \begin{pmatrix} \langle b_{v\mathbf{r}\uparrow} \rangle \\ \langle b_{v\mathbf{r}\downarrow} \rangle \end{pmatrix} \\ &= \begin{pmatrix} z_2 & -\frac{i}{\sqrt{2}}w_1 - \frac{1}{\sqrt{2}}w_2 \\ -w_2^* & \frac{i}{\sqrt{2}}z_1^* - \frac{1}{\sqrt{2}}z_2^* \end{pmatrix} \begin{pmatrix} e^{i\mathbf{Q}\cdot\mathbf{r}} \\ e^{-i\mathbf{Q}\cdot\mathbf{r}} \end{pmatrix}. \end{aligned} \quad (\text{C17})$$

In order to have uniform magnitude for the ordered moments $(1/2)x_{u,v}^\dagger x_{u,v}$, we have to impose the constraint $x_u^\dagger x_u = x_v^\dagger x_v = \text{const}$.

From (C16) and (C17) we find that there are four distinct spinors in a plaquette which are named as \mathcal{Z}_1 if x is even and y is even, \mathcal{Z}_2 if x is odd and y is even, \mathcal{Z}_3 if x is odd and y is odd and \mathcal{Z}_4 if x is even and y is odd. Only two of them are linearly independent.

Therefore we choose two linearly independent spinors as:

$$\psi = \mathcal{Z}_1 = \begin{pmatrix} z_1 - \frac{i}{\sqrt{2}}w_1 - \frac{1}{\sqrt{2}}w_2 \\ -w_1^* - \frac{i}{\sqrt{2}}z_1^* - \frac{1}{\sqrt{2}}z_2^* \end{pmatrix} \quad (\text{C18})$$

$$i\chi = \mathcal{Z}_2 = i \begin{pmatrix} z_2 + \frac{i}{\sqrt{2}}w_1 + \frac{1}{\sqrt{2}}w_2 \\ -w_2^* + \frac{i}{\sqrt{2}}z_1^* + \frac{1}{\sqrt{2}}z_2^* \end{pmatrix} \quad (\text{C19})$$

$$(\text{C20})$$

Therefore \mathcal{Z}_3 and \mathcal{Z}_4 can be represented as:

$$\mathcal{Z}_3 = \begin{pmatrix} z_2 + \frac{1}{\sqrt{2}}w_1 + \frac{i}{\sqrt{2}}w_2 \\ -w_2^* + \frac{1}{\sqrt{2}}z_1^* + \frac{i}{\sqrt{2}}z_2^* \end{pmatrix} \quad (\text{C21})$$

$$= -\sqrt{2}i\sigma_y\psi^* + i\chi, \quad (\text{C22})$$

$$\mathcal{Z}_4 = i \begin{pmatrix} z_2 - \frac{1}{\sqrt{2}}w_1 - \frac{i}{\sqrt{2}}w_2 \\ -w_2^* - \frac{1}{\sqrt{2}}z_1^* - \frac{i}{\sqrt{2}}z_2^* \end{pmatrix} \quad (\text{C23})$$

$$= \sqrt{2}i\sigma_y\chi^* + i\psi. \quad (\text{C24})$$

The constraints that condensate on every site is uniform require that

$$|\psi|^2 = |i\chi|^2 = |-\sqrt{2}i\sigma_y\psi^* + i\chi|^2 = |\sqrt{2}i\sigma_y\chi^* + i\psi|^2. \quad (\text{C25})$$

The constraints can be simplified if we define two spinors

$$\phi_+ = \sqrt{2 + \sqrt{2}}(\psi + \sigma_y\chi^*), \quad (\text{C26})$$

$$\phi_- = \sqrt{2 - \sqrt{2}}(\psi - \sigma_y\chi^*). \quad (\text{C27})$$

Therefore we have:

$$\mathcal{Z}_1 = \frac{1}{2\sqrt{2}}(\sqrt{2 - \sqrt{2}}\phi_+ + \sqrt{2 + \sqrt{2}}\phi_-), \quad (\text{C28})$$

$$\mathcal{Z}_2 = \frac{1}{2\sqrt{2}}i\sigma_y(-\sqrt{2 - \sqrt{2}}\phi_+^* + \sqrt{2 + \sqrt{2}}\phi_-^*) \quad (\text{C29})$$

$$\mathcal{Z}_3 = \frac{1}{2\sqrt{2}}i\sigma_y(-\sqrt{2 + \sqrt{2}}\phi_+^* - \sqrt{2 - \sqrt{2}}\phi_-^*) \quad (\text{C30})$$

$$\mathcal{Z}_4 = \frac{1}{2\sqrt{2}}(\sqrt{2 + \sqrt{2}}\phi_+ - \sqrt{2 - \sqrt{2}}\phi_-). \quad (\text{C31})$$

And the constraints now become

$$|\phi_+|^2 = |\phi_-|^2, \quad \text{Re}(\phi_+^\dagger\phi_-) = 0. \quad (\text{C32})$$

Define vector order parameter on the four sites as $\vec{n}_i = \mathcal{Z}_i^\dagger \sigma \mathcal{Z}_i$, ($i = 1, 2, 3, 4$). It is easy to verify that $\sum_i \vec{n}_i = 0$.

Therefore we can parameterize vector order parameter on every site as:

$$\vec{n} = (-)^x \vec{n}_{(\pi,0)} + (-)^y \vec{n}_{(0,\pi)} + (-)^{x+y} \vec{n}_{(\pi,\pi)}. \quad (\text{C33})$$

The three vectors, $\vec{n}_{(\pi,0)}$, $\vec{n}_{(0,\pi)}$ and $\vec{n}_{(\pi,\pi)}$, corresponds to \mathbf{m}_1 , \mathbf{m}_2 and \mathbf{m}_3 in main text respectively.

The three order parameters $\vec{n}_{(\pi,0)}$, $\vec{n}_{(0,\pi)}$ and $\vec{n}_{(\pi,\pi)}$ can be represented with two spinors ϕ_+ and ϕ_-

$$\begin{aligned} \vec{n}_{(\pi,0)} &= ((\vec{n}_1 + \vec{n}_4) - (\vec{n}_2 + \vec{n}_3))/4 \\ &= \frac{1}{4}(\vec{n}_{\phi_+} + \vec{n}_{\phi_-}), \\ \vec{n}_{(0,\pi)} &= ((\vec{n}_1 + \vec{n}_2) - (\vec{n}_3 + \vec{n}_4))/4 \\ &= \frac{\sqrt{2}}{8}(\phi_+^\dagger \vec{\sigma} \phi_- + \phi_-^\dagger \vec{\sigma} \phi_+), \\ \vec{n}_{(\pi,\pi)} &= ((\vec{n}_1 + \vec{n}_3) - (\vec{n}_2 + \vec{n}_4))/4 \\ &= \frac{\sqrt{2}}{8}(-\vec{n}_{\phi_+} + \vec{n}_{\phi_-}), \end{aligned} \quad (\text{C34})$$

where we have defined $\vec{n}_{\phi_\pm} = \phi_\pm^\dagger \vec{\sigma} \phi_\pm$.

The manifold of the order parameter can be described as follows. Given two spinors ϕ_+ and ϕ_- with the same magnitude, we can perform SU(2) transformations to them separately without altering the condition $|\phi_+|^2 = |\phi_-|^2$. And then we can tune the relative U(1) phase between the two spinors to meet the condition $\text{Re}(\phi_+^\dagger\phi_-) = 0$.

In principle, the transformation rule of the spinor fields ϕ_+ and ϕ_- under space group operation can be worked out through the corresponding transformation rule of bosonic field under PSG.

It is easy to deduce from constraints (C25) that the intersection angle between magnetic moments on neighboring sites should always be greater than 90° . And note that the Néel state is not forbidden by this condition and therefore is one of possible magnetic ordered states that can be obtained from the π -flux state through boson condensation.

Appendix D: Derivation of the continuum-field theory for the transition from Z_2 spin liquid states to Néel ordered states

In this Appendix we derive the continuum-field theory for the two Z_2 spin liquid states from the microscopic Hamiltonian in the long wavelength limit.

We divide sublattice u and v with different parity $(-)^{x+y}$: u sublattice is parity-even and v is parity-odd.

Following Read and Sachdev's prescription⁴⁵, we represent the boson operator in terms of the two slow-varying fields

$$\begin{aligned} b_{u,\mathbf{r},\alpha} &= \psi_{u,\alpha}(\mathbf{r})e^{iQ\cdot\mathbf{r}}, \\ b_{v,\mathbf{r},\alpha} &= -\sigma_{\alpha\beta}^y \psi_{v,\beta}^*(\mathbf{r})e^{iQ\cdot\mathbf{r}}, \end{aligned} \quad (\text{D1})$$

where Q represents the k point where condensation of bosons happens.

The bond operator $\hat{A}_1, \hat{B}_1, \hat{B}_2$ therefore can be represented as: Nearest bond \hat{A}_1 :

$$\begin{aligned} \hat{A}_{\mathbf{r},\mathbf{r}'} &= \frac{1}{2}(b_{u,\mathbf{r},\uparrow}b_{v,\mathbf{r}',\downarrow} - b_{u,\mathbf{r},\downarrow}b_{v,\mathbf{r}',\uparrow}) \\ &= -\frac{i}{2}e^{iQ\cdot\Delta\mathbf{r}}\psi_{u,\alpha}[1 + \Delta\mathbf{r} \cdot \partial_{\mathbf{r}} + \frac{(\Delta\mathbf{r} \cdot \partial_{\mathbf{r}})^2}{2} + \dots]\psi_{v,\alpha}^*. \end{aligned} \quad (\text{D2})$$

Nearest bond \hat{B}_1 :

$$\begin{aligned} \hat{B}_{\mathbf{r},\mathbf{r}'} &= \frac{1}{2}b_{u,\mathbf{r},\alpha}^\dagger b_{v,\mathbf{r}',\alpha} \\ &= -\frac{1}{2}e^{iQ\cdot\Delta\mathbf{r}}\sigma_{\alpha\beta}^y \psi_{u,\alpha}^*[1 + \Delta\mathbf{r} \cdot \partial_{\mathbf{r}} + \frac{(\Delta\mathbf{r} \cdot \partial_{\mathbf{r}})^2}{2} + \dots]\psi_{v,\beta}. \end{aligned} \quad (\text{D3})$$

Nex-nearest bond \hat{B}_2 :

$$\begin{aligned} &\frac{1}{2}b_{u,\mathbf{r},\alpha}^\dagger b_{u,\mathbf{r}',\alpha} \\ &= \frac{1}{2}e^{iQ\cdot\Delta\mathbf{r}}\psi_{u,\alpha}^*[1 + \Delta\mathbf{r} \cdot \partial_{\mathbf{r}} + \frac{(\Delta\mathbf{r} \cdot \partial_{\mathbf{r}})^2}{2} + \dots]\psi_{u,\alpha}, \end{aligned} \quad (\text{D4})$$

and

$$\begin{aligned} & \frac{1}{2}b_{v,r,\alpha}^\dagger b_{v,r',\alpha} \\ &= \frac{1}{2}e^{iQ \cdot \Delta \mathbf{r}} \psi_{v,\alpha}^* [1 + \Delta \mathbf{r} \cdot \partial_{\mathbf{r}} + \frac{(\Delta \mathbf{r} \cdot \partial_{\mathbf{r}})^2}{2} + \dots] \psi_{v,\alpha}, \end{aligned} \quad (\text{D5})$$

where $\Delta \mathbf{r} = \mathbf{r}' - \mathbf{r}$.

1. $Z_2[0,0]$ state

The minima are located at $\pm(\pi/2, -\pi/2)$. Therefore we choose $Q = (\pi/2, -\pi/2)$ in (D1).

Inserting (D2)-(D4) into the mean-field Hamiltonian (22), we obtain:

$$\begin{aligned} \mathcal{L} = & \int \frac{d^2 \mathbf{r}}{a^2} \left\{ \psi_{u,\alpha}^* \frac{d}{d\tau} \psi_{u,\alpha} - \psi_{v,\alpha}^* \frac{d}{d\tau} \psi_{v,\alpha} - \mu (\psi_{u,\alpha}^* \psi_{u,\alpha} \right. \\ & + \psi_{v,\alpha}^* \psi_{v,\alpha}) - 2A_1 \psi_{u,\alpha} \psi_{v,\alpha}^* + \frac{a^2}{2} A_1 \partial_{\mathbf{r}} \psi_{u,\alpha} \cdot \partial_{\mathbf{r}} \psi_{v,\alpha}^* + c.c. \\ & - 2B_1^* i \sigma_{\alpha\beta}^y \psi_{u,\alpha}^* \psi_{v,\beta}^* + \frac{a^2}{2} B_1^* i \sigma_{\alpha\beta}^y \partial_{\mathbf{r}} \psi_{u,\alpha}^* \cdot \partial_{\mathbf{r}} \psi_{v,\beta}^* + c.c. \\ & + 2B_2 (\psi_{u,\alpha}^* \psi_{u,\alpha} + \psi_{v,\alpha}^* \psi_{v,\alpha}) - a^2 B_2 (\partial_{\mathbf{r}} \psi_{u,\alpha}^* \cdot \partial_{\mathbf{r}} \psi_{u,\alpha} \\ & \left. + \partial_{\mathbf{r}} \psi_{v,\alpha}^* \cdot \partial_{\mathbf{r}} \psi_{v,\alpha}) \right\}. \end{aligned} \quad (\text{D6})$$

Note that terms with odd spatial derivatives vanish due to the geometry of the square lattice.

Introduce two fields:

$$z_\alpha = (\psi_{u,\alpha} + \psi_{v,\alpha})/2, \pi_\alpha = (\psi_{u,\alpha} - \psi_{v,\alpha})/2. \quad (\text{D7})$$

The Lagrangian now becomes

$$\begin{aligned} \mathcal{L} = & \int \frac{d^2 \mathbf{r}}{a^2} \left\{ 2z_\alpha^* \frac{d}{d\tau} \pi_\alpha + 2\pi_\alpha^* \frac{d}{d\tau} z_\alpha \right. \\ & + (-2\mu - 4A_1 + 4B_2) z_\alpha^* z_\alpha + (-2\mu + 4A_1 + 4B_2) \pi_\alpha^* \pi_\alpha \\ & + a^2 (A_1 - 2B_2) \partial_{\mathbf{r}} z_\alpha^* \cdot \partial_{\mathbf{r}} z_\alpha \\ & \left. - a^2 B_1^* i \sigma_{\alpha\beta}^y \partial_{\mathbf{r}} z_\alpha^* \cdot \partial_{\mathbf{r}} \pi_\beta^* + c.c. + 4B_1^* z_\alpha^* i \sigma_{\alpha\beta}^y \pi_\beta^* + c.c. \right\}, \end{aligned} \quad (\text{D8})$$

where terms involving π field and spatial derivatives are omitted since they will generate terms with fourth or higher power of spatial derivatives of z field after integrating out π field.

Fields π_α have a large mass gap $-2\mu + 4A_1 + 4B_2$ and can be safely integrated out. The low energy effective Lagrangian after integration is :

$$\begin{aligned} \mathcal{L} = & \int d^2 \mathbf{r} \left\{ \frac{2}{(-\mu + 2A_1 + 2B_2)a^2} \partial_\tau z_\alpha^* \cdot \partial_\tau z_\alpha \right. \\ & + (A_1 - 2B_2 + \frac{4|B_1|^2}{-\mu + 2A_1 + 2B_2}) \partial_{\mathbf{r}} z_\alpha^* \cdot \partial_{\mathbf{r}} z_\alpha \\ & + \left(\frac{-2\mu - 4A_1 + 4B_2}{a^2} - \frac{8}{(-\mu + 2A_1 + 2B_2)a^2} |B_1|^2 \right) z_\alpha^* z_\alpha \\ & \left. + \frac{4}{(-\mu + 2A_1 + 2B_2)a^2} B_1 \frac{d}{d\tau} z_\alpha i \sigma_{\alpha\beta}^y z_\beta + c.c. \right\}. \end{aligned} \quad (\text{D9})$$

Note that the Higgs term $B_1 \frac{d}{d\tau} z_\alpha i \sigma_{\alpha\beta}^y z_\beta + c.c.$ plays the role of the vector spin chirality order parameter for reasons discussed in the text.

The Lagrangian can be further simplified after introducing two fields ω_α , $\alpha = 1, 2$ (here we assume $\text{Im}(B_1) > 0$),

$$\begin{aligned} \omega_1 &= \frac{z_\uparrow + z_\downarrow + i(z_\uparrow^* - z_\downarrow^*)}{2}, \\ \omega_2 &= \frac{z_\uparrow^* + z_\downarrow^* + i(z_\uparrow - z_\downarrow)}{2}, \end{aligned} \quad (\text{D10})$$

and has the form

$$\begin{aligned} \mathcal{L} = & \int d^2 \mathbf{r} \left\{ \frac{2}{(-\mu + 2A_1 + 2B_2)a^2} \partial_\tau \omega_\alpha^* \cdot \partial_\tau \omega_\alpha \right. \\ & + (A_1 - 2B_2 + \frac{4|B_1|^2}{-\mu + 2A_1 + 2B_2}) \partial_{\mathbf{r}} \omega_\alpha^* \cdot \partial_{\mathbf{r}} \omega_\alpha \\ & + \left(\frac{-2\mu - 4A_1 + 4B_2}{a^2} - \frac{8}{(-\mu + 2A_1 + 2B_2)a^2} |B_1|^2 \right) \omega_\alpha^* \omega_\alpha \\ & \left. + \frac{8}{(-\mu + 2A_1 + 2B_2)a^2} \text{Im}(B_1) \omega_\alpha^* \frac{d}{d\tau} \omega_\alpha \right\}. \end{aligned} \quad (\text{D11})$$

Therefore the Lagrangian will flow to a new fixed point where space and time scales differently. The dispersion relation is now $\omega \propto k^2$ with dynamical critical component $z = 2$.

The term with quadratic powers of time derivatives is irrelevant and hence can be dropped.

2. $Z_2[0,\pi]$ state

In this case the minima of the spinon dispersion are located at $\pm Q$ where $Q = (\pi/2, \pi/2)$.

Inserting (D2)-(D4) into the mean field Hamiltonian,

we therefore obtain:

$$\begin{aligned}
\mathcal{L} = & \int \frac{d^2\mathbf{r}}{a^2} \{ \psi_{u,\alpha}^* \frac{d}{d\tau} \psi_{u,\alpha} - \psi_{v,\alpha}^* \frac{d}{d\tau} \psi_{v,\alpha} - \mu (\psi_{u,\alpha}^* \psi_{u,\alpha} \\
& + \psi_{v,\alpha}^* \psi_{v,\alpha}) - 2A_1 \psi_{u,\alpha} \psi_{v,\alpha}^* + \frac{a^2}{2} A_1 \partial_{\mathbf{r}} \psi_{u,\alpha} \cdot \partial_{\mathbf{r}} \psi_{v,\alpha}^* + c.c. \\
& + \frac{a^2}{2} B_1^* i \sigma_{\alpha\beta}^y \psi_{u,\alpha}^* [\partial_y^2 - \partial_x^2] \psi_{v,\beta} + c.c. \\
& - 2B_2 (\psi_{u,\alpha}^* \psi_{u,\alpha} + \psi_{v,\alpha}^* \psi_{v,\alpha}) + a^2 B_2 (\partial_{\mathbf{r}} \psi_{u,\alpha}^* \cdot \partial_{\mathbf{r}} \psi_{u,\alpha} \\
& + \partial_{\mathbf{r}} \psi_{v,\alpha}^* \cdot \partial_{\mathbf{r}} \psi_{v,\alpha}) \}. \tag{D12}
\end{aligned}$$

Introduce two fields z and π defined in (D7), the Lagrangian becomes:

$$\begin{aligned}
\mathcal{L} = & \int \frac{d^2\mathbf{r}}{a^2} \{ 2z_{\alpha}^* \frac{d}{d\tau} \pi_{\alpha} + 2\pi_{\alpha}^* \frac{d}{d\tau} z_{\alpha} \\
& + (-2\mu - 4A_1 - 4B_2) z_{\alpha}^* z_{\alpha} + (-2\mu + 4A_1 - 4B_2) \pi_{\alpha}^* \pi_{\alpha} \\
& + a^2 (A_1 + 2B_2) \partial_{\mathbf{r}} z_{\alpha}^* \cdot \partial_{\mathbf{r}} z_{\alpha} \\
& - a^2 B_1^* i \sigma_{\alpha\beta}^y z_{\alpha}^* [\partial_y^2 - \partial_x^2] \pi_{\beta}^* + c.c. \}. \tag{D13}
\end{aligned}$$

After integrating out π field, we obtain a low energy effective Lagrangian:

$$\begin{aligned}
\mathcal{L} = & \int d^2\mathbf{r} \{ \frac{2}{(-\mu + 2A_1 - 2B_2)a^2} \partial_{\mathbf{r}} z_{\alpha}^* \cdot \partial_{\mathbf{r}} z_{\alpha} \\
& + (A_1 + 2B_2) \partial_{\mathbf{r}} z_{\alpha}^* \cdot \partial_{\mathbf{r}} z_{\alpha} + \frac{(-2\mu - 4A_1 - 4B_2)}{a^2} z_{\alpha}^* z_{\alpha} \}. \tag{D14}
\end{aligned}$$

Here the Higgs terms consist of B_1 have cubic powers of time and spatial derivatives or higher and hence is irrelevant by naive power counting.

After rescaling and restore the compact gauge field, we obtain an effective field theory consists of a massive boson z_{α} coupled to a compact U(1) gauge field,

$$\mathcal{L} = \int d^2\mathbf{r} [|D_{\tau} z|^2 + c^2 |D_{\mathbf{r}} z|^2 + m^2 |z|^2]. \tag{D15}$$

The critical point of this theory is $\mu = -2A_1 - 2B_2$ consistent with the mean field solution and the spinon velocity c is proportional to $\sqrt{A_1(A_1 + 2B_2)}$.

Appendix E: Calculation of vison PSG

In this section we will derive the vison PSG for square lattice⁴⁰⁻⁴⁴.

The dynamics of vison can be described by an odd Ising gauge theory in the dimer limit. After a duality transformation, the odd Ising gauge theory is transformed to a transverse field Ising model on the dual lattice.

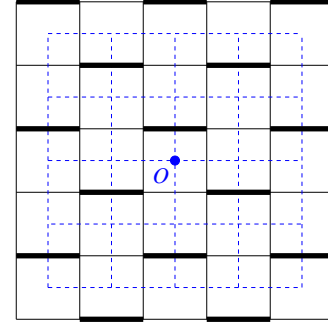


FIG. 13: Gauge choice on the dual lattice (solid black lines). The vison hopping J_{ij} on the thick bonds are negative. The blue dashed line represents the original lattice. Note that all the point group symmetry operations are defined with respect to the original lattice site O .

Following Ref. 44, the dynamics of vison can be described by a fully frustrated transverse-field Ising theory on the dual lattice.

$$H = \sum_{ij} J_{ij} \tau_i^z \tau_j^z - \sum_i K_i \tau_i^x \dots, \tag{E1}$$

where the product of bonds around each elementary plaquette is

$$\prod_{\text{plaquette}} \text{sgn}(J_{ij}) = -1. \tag{E2}$$

This Hamiltonian is invariant under Z_2 gauge transformation

$$\tau_i \rightarrow \eta_i \tau_i, K_i \rightarrow \eta_i K_i, J_{ij} \rightarrow \eta_i \eta_j J_{ij}, \tag{E3}$$

where $\eta_i = \pm 1$.

Due to the Z_2 gauge structure, we adopt a specific gauge choice (FIG. 13) for J_{ij} and calculate the vison PSG under this gauge.

In the following we shall ignore the kinetic term $K_i \tau_i^x$ and adopt a soft-spin formulation where the vison field τ_i^z 's take real values. Considering nearest and fourth nearest neighbor interaction of the vison fields as considered in Ref. 44, there are eight (rather than 4 because two sets of sublattice are not equivalent) inequivalent minimal points in the Brillouin zone (see Fig. 14).

$$\begin{aligned}
Q_1 = (0, 0), Q_2 = (0, \pi), Q_3 = \left(\frac{\pi}{2}, \frac{\pi}{2}\right), Q_4 = \left(\frac{\pi}{2}, \frac{\pi}{2}\right), \\
Q_{1'} = (\pi, \pi), Q_{2'} = (\pi, 0), Q_{3'} = \left(\frac{\pi}{2}, \frac{-\pi}{2}\right), Q_{4'} = \left(-\frac{\pi}{2}, -\frac{\pi}{2}\right) \tag{E4}
\end{aligned}$$

Expand the vison field with slow varying modes ϕ_a ($a = 1, 2, 3, 4, 1', 2', 3', 4'$) at these eight momenta:

$$\tau^z = \sum_a \phi_a e^{i\vec{Q}_a \cdot \vec{r}}. \tag{E5}$$

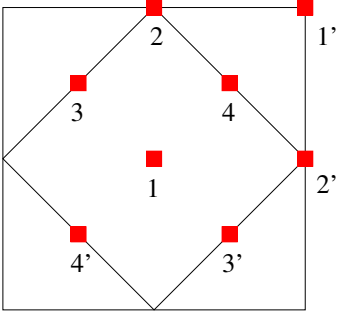


FIG. 14: Brillouin zone of the square lattice, and the eight momenta, labeled as 1, 2, 3, 4, 1', 2', 3', 4' and indicated by red squares in the figure, for low energy vison modes.

Under symmetry operation, the vison fields transform as

$$T_1 : \tau_{x,y}^z \rightarrow (-)^{x+1} \tau_{x+1,y}^z, \quad (\text{E6})$$

$$T_2 : \tau_{x,y}^z \rightarrow (-)^x \tau_{x,y+1}^z, \quad (\text{E7})$$

$$P_x : \tau_{x,y}^z \rightarrow (-)^x \tau_{x,1-y}^z, \quad (\text{E8})$$

$$P_y : \tau_{x,y}^z \rightarrow \tau_{1-x,y}^z, \quad (\text{E9})$$

$$P_{xy} : \tau_{x,y}^z \rightarrow \frac{(1-i)i^{x+y} + (1+i)i^{-x-y}}{2} \tau_{y,x}^z. \quad (\text{E10})$$

We choose base functions as $(\phi_1, \phi_2, \phi_3, \phi_4, \phi_{1'}, \phi_{2'}, \phi_{3'}, \phi_{4'})^T$, the vison modes transform under symmetry operation as

$$\phi_n \rightarrow \sum_{m=1}^8 [O_\phi(g)]_{n,m} \phi_m. \quad (\text{E11})$$

Therefore we can directly write out the transformation matrices

$$O_\phi(T_1) = \begin{pmatrix} 0 & 0 & 0 & 0 & 0 & -1 & 0 & 0 \\ 0 & 0 & 0 & 0 & -1 & 0 & 0 & 0 \\ 0 & 0 & 0 & i & 0 & 0 & 0 & 0 \\ 0 & 0 & -i & 0 & 0 & 0 & 0 & 0 \\ 0 & 1 & 0 & 0 & 0 & 0 & 0 & 0 \\ 1 & 0 & 0 & 0 & 0 & 0 & 0 & 0 \\ 0 & 0 & 0 & 0 & 0 & 0 & 0 & -i \\ 0 & 0 & 0 & 0 & 0 & 0 & i & 0 \end{pmatrix}, \quad (\text{E12})$$

$$O_\phi(T_2) = \begin{pmatrix} 0 & 0 & 0 & 0 & 0 & 1 & 0 & 0 \\ 0 & 0 & 0 & 0 & -1 & 0 & 0 & 0 \\ 0 & 0 & 0 & i & 0 & 0 & 0 & 0 \\ 0 & 0 & i & 0 & 0 & 0 & 0 & 0 \\ 0 & -1 & 0 & 0 & 0 & 0 & 0 & 0 \\ 1 & 0 & 0 & 0 & 0 & 0 & 0 & 0 \\ 0 & 0 & 0 & 0 & 0 & 0 & 0 & -i \\ 0 & 0 & 0 & 0 & 0 & 0 & -i & 0 \end{pmatrix}, \quad (\text{E13})$$

$$O_\phi(P_x) = \begin{pmatrix} 0 & 0 & 0 & 0 & 0 & 1 & 0 & 0 \\ 0 & 0 & 0 & 0 & -1 & 0 & 0 & 0 \\ 0 & 0 & 0 & 0 & 0 & 0 & i & 0 \\ 0 & 0 & 0 & 0 & 0 & 0 & 0 & i \\ 0 & -1 & 0 & 0 & 0 & 0 & 0 & 0 \\ 1 & 0 & 0 & 0 & 0 & 0 & 0 & 0 \\ 0 & 0 & -i & 0 & 0 & 0 & 0 & 0 \\ 0 & 0 & 0 & -i & 0 & 0 & 0 & 0 \end{pmatrix}, \quad (\text{E14})$$

$$O_\phi(P_y) = \begin{pmatrix} 1 & 0 & 0 & 0 & 0 & 0 & 0 & 0 \\ 0 & 1 & 0 & 0 & 0 & 0 & 0 & 0 \\ 0 & 0 & 0 & -i & 0 & 0 & 0 & 0 \\ 0 & 0 & i & 0 & 0 & 0 & 0 & 0 \\ 0 & 0 & 0 & 0 & -1 & 0 & 0 & 0 \\ 0 & 0 & 0 & 0 & 0 & -1 & 0 & 0 \\ 0 & 0 & 0 & 0 & 0 & 0 & 0 & i \\ 0 & 0 & 0 & 0 & 0 & 0 & -i & 0 \end{pmatrix}, \quad (\text{E15})$$

$$O_\phi(P_{xy}) = \frac{1}{2} \begin{pmatrix} 0 & 0 & 0 & 1-i & 0 & 0 & 0 & 1+i \\ 0 & 0 & 1-i & 0 & 0 & 0 & 1+i & 0 \\ 0 & 1+i & 0 & 0 & 0 & 1-i & 0 & 0 \\ 1+i & 0 & 0 & 0 & 1-i & 0 & 0 & 0 \\ 0 & 0 & 0 & 1+i & 0 & 0 & 0 & 1-i \\ 0 & 0 & 1+i & 0 & 0 & 0 & 1-i & 0 \\ 0 & 1-i & 0 & 0 & 0 & 1+i & 0 & 0 \\ 1-i & 0 & 0 & 0 & 1+i & 0 & 0 & 0 \end{pmatrix}. \quad (\text{E16})$$

In the following we may identify the operation P_x with σ and $P_{xy}P_x$ with C_4 , therefore

$$O_\phi(C_4) = O_\phi(P_{xy})O_\phi(P_x) = \frac{1}{2} \begin{pmatrix} 0 & 0 & 0 & 1-i & 0 & 0 & 0 & 1+i \\ 0 & 0 & 1-i & 0 & 0 & 0 & 1+i & 0 \\ 1-i & 0 & 0 & 0 & -1-i & 0 & 0 & 0 \\ 0 & -1+i & 0 & 0 & 0 & 1+i & 0 & 0 \\ 0 & 0 & 0 & -1-i & 0 & 0 & 0 & -1+i \\ 0 & 0 & -1-i & 0 & 0 & 0 & -1+i & 0 \\ 1+i & 0 & 0 & 0 & -1+i & 0 & 0 & 0 \\ 0 & -1-i & 0 & 0 & 0 & 1-i & 0 & 0 \end{pmatrix}. \quad (\text{E17})$$

The vison PSGs now can be easily obtained:

$$\begin{aligned} O_\phi(T_2)^{-1}O_\phi(T_1)O_\phi(T_2)O_\phi(T_1)^{-1} &= -1, \\ O_\phi(\sigma)^{-1}O_\phi(T_1)O_\phi(\sigma)O_\phi(T_1)^{-1} &= -1, \\ O_\phi(\sigma)^{-1}O_\phi(T_2)O_\phi(\sigma)O_\phi(T_2) &= 1, \\ O_\phi(\sigma)^2 &= 1, \\ O_\phi(\sigma)^{-1}O_\phi(C_4)O_\phi(\sigma)O_\phi(C_4) &= 1, \\ O_\phi(C_4)^4 &= -1, \\ O_\phi(C_4)^{-1}O_\phi(T_1)O_\phi(C_4)O_\phi(T_2) &= -1, \\ O_\phi(C_4)^{-1}O_\phi(T_2)O_\phi(C_4)O_\phi(T_1)^{-1} &= 1. \end{aligned} \quad (\text{E18})$$

Appendix F: Solutions of Abrikosov fermion PSG

The Abrikosov fermion PSG on square lattice are studied in great detail in Ref. 27. In this Appendix, we briefly summarize the algebraic solutions of fermionic PSGs and introduce some notations for convenience.

The solutions to the fermionic PSGs are as follows:

$$G_{T_x}(\mathbf{i}) = \eta_{xy}^{i_y} \tau_0, \quad (\text{F1})$$

$$G_{T_y}(\mathbf{i}) = \tau_0, \quad (\text{F2})$$

$$G_{P_x}(\mathbf{i}) = \eta_{xpx}^{i_x} \eta_{xpy}^{i_y} g_{P_x}, \quad (\text{F3})$$

$$G_{P_y}(\mathbf{i}) = \eta_{xpy}^{i_x} \eta_{xpx}^{i_y} g_{P_y}, \quad (\text{F4})$$

$$G_{P_{xy}}(\mathbf{i}) = \eta_{xy}^{i_x i_y} g_{P_{xy}}, \quad (\text{F5})$$

$$G_{\mathcal{T}}(\mathbf{i}) = \eta_t^{i_x + i_y} g_{\mathcal{T}}. \quad (\text{F6})$$

In Wen's notation, $T_{x,y}$ stands for translation symmetry, and three parity operations P_x , P_y and P_{xy} acts as follows:

$$P_x : (i_x, i_y) \rightarrow (-i_x, i_y), \quad (\text{F7})$$

$$P_y : (i_x, i_y) \rightarrow (i_x, -i_y), \quad (\text{F8})$$

$$P_{xy} : (i_x, i_y) \rightarrow (i_y, i_x). \quad (\text{F9})$$

stands for reflection along y axis, reflection along x axis and respectively.

Note that $C_4 = P_{xy}P_y$, therefore we can obtain the PSG for C_4 from the product of P_{xy} and P_y . And the σ operation is just the operation P_y in Wen's notation.

The fermionic PSGs are characterized by four numbers: $\eta_{xpx}, \eta_{xpy}, \eta_{xy}, \eta_t$, and numbers from the commutative relations of $SU(2)$ matrices as defined in TABLE VII.

Algebraic Identities	Z_2 numbers from commutative relations
$\sigma^2 = 1$	$[g_{P_y}]^2 = \eta_\sigma$
$\sigma^{-1}C_4\sigma C_4 = 1$	$[g_{P_y}]^{-1}[g_{P_{xy}}g_{P_y}][g_{P_y}][g_{P_{xy}}g_{P_y}] = \eta_\sigma C_4$
$C_4^4 = 1$	$[g_{P_{xy}}g_{P_y}]^4 = \eta_{C_4}$
$C_4^{-1}\mathcal{T}^{-1}C_4\mathcal{T} = 1$	$[g_{P_{xy}}g_{P_y}]^{-1}g_{\mathcal{T}}^{-1}g_{P_{xy}}g_{P_y}g_{\mathcal{T}} = \eta_{C_4}\mathcal{T}$
$\sigma^{-1}\mathcal{T}^{-1}\sigma\mathcal{T} = 1$	$g_{P_y}^{-1}g_{\mathcal{T}}^{-1}g_{P_y}g_{\mathcal{T}} = \eta_\sigma\mathcal{T}$

TABLE VII: Z_2 numbers from the commutative relations between $SU(2)$ matrices. Here η_i are numbers that can be ± 1 , and g_i are $SU(2)$ matrices as defined in Eq. (F1)-(F6).

Appendix G: Physical realization of Abrikosov fermion spin liquid states

In this Appendix we will analyze the physical realization of the fermionic PSGs as shown in TABLE III. As discussed in Ref. 27, the mean-field ansatz U_{ij} should take the form of

$$U_{ij} = i\rho_{ij}W_{ij}, \quad (\text{G1})$$

(here ρ_{ij} is a non-negative real number, and $W_{ij} \in SU(2)$) in order to describe a spin-rotational symmetric fermionic spin liquid state, and the time-reversal symmetry \mathcal{T} is implemented as

$$\mathcal{T} : U_{ij} \rightarrow -U_{ij}. \quad (\text{G2})$$

The symmetry operations are defined in Eq. (F7)-(F9).

1. Realization of the $Z_2 B \tau_-^1 \tau_-^1 \tau_-^1 \tau_-^3$ state

PSG elements of this state are:

$$G_x(i) = (-)^{iy} \tau_0; \quad (\text{G3})$$

$$G_y(i) = \tau_0; \quad (\text{G4})$$

$$G_{P_x}(i) = (-)^{ix+iy} i \tau_1; \quad (\text{G5})$$

$$G_{P_y}(i) = (-)^{ix+iy} i \tau_1; \quad (\text{G6})$$

$$G_{P_{xy}}(i) = (-)^{ix+iy} i \tau_1; \quad (\text{G7})$$

$$G_{\mathcal{T}}(i) = (-)^{ix+iy} i \tau_3. \quad (\text{G8})$$

There are two sites in a unit cell of π -flux fermionic spin liquid states distinguished by parity $(-)^x = \pm 1$, which are labeled by u and v respectively.

First, let us consider the Lagrangian multiplier a_0^l . Since the term $a_0^l \tau_l$ should be invariant under $G_{\mathcal{T}\mathcal{T}}$, we have $\{a_0^l \tau_l, \tau_3\} = 0$. And it is also invariant under $G_{P_x} P_x, G_{P_y} P_y$ and $G_{P_{xy}} P_{xy}$, so we have $[a_0^l \tau_l, \tau_1] = 0$. Hence we have $a_0^1 \neq 0$ and $a_0^{2,3} = 0$.

a. Nearest-neighbor bond

With translation along x and y direction, we can write down the general form of the nearest bonds:

$$U_{i,i+\hat{x}} = u_{\hat{x}}, \quad (\text{G9})$$

$$U_{i,i+\hat{y}} = (-)^{ix} u_{\hat{y}}, \quad (\text{G10})$$

where $u_{\hat{x}}$ and $u_{\hat{y}}$ are site-independent.

Since $u_{\hat{x}}$ is invariant under time-reversal operation, we have $G_{\mathcal{T}}(i) u_{\hat{x}} G_{\mathcal{T}}^\dagger(i + \hat{x}) = -u_{\hat{x}}$, which leads to $[u_{\hat{x}}, \tau_3] = 0$.

$u_{\hat{x}}$ is also invariant under P_y : $G_{P_y}(i) u_{\hat{x}} G_{P_y}^\dagger(i + \hat{x}) = u_{\hat{x}}$, therefore $\{u_{\hat{x}}, \tau_1\} = 0$. Hence we have

$$u_{\hat{x}} = \eta \tau_3. \quad (\text{G11})$$

Under P_{xy} , $G_{P_{xy}}(i) u_{\hat{x}} G_{P_{xy}}^\dagger(i + \hat{x}) = (-)^{iy} u_{\hat{y}}$, therefore

$$u_{\hat{y}} = -\eta \tau_3. \quad (\text{G12})$$

b. Next-nearest-neighbor bond

The general form of the bonds is:

$$U_{i,i+\hat{x}+\hat{y}} = (-)^{ix} u_{\hat{x}+\hat{y}}, \quad (\text{G13})$$

$$U_{i,i+\hat{x}-\hat{y}} = (-)^{ix} u_{\hat{x}-\hat{y}}. \quad (\text{G14})$$

Under $P_x P_y$, we have

$$\begin{aligned} G_{P_x} P_x G_{P_y} P_y U_{O,O+\hat{x}+\hat{y}} [G_{P_x} P_x G_{P_y} P_y]^\dagger \\ = U_{O,O-\hat{x}-\hat{y}}, \end{aligned} \quad (\text{G15})$$

where O represents the original point.

Therefore we have

$$u_{\hat{x}+\hat{y}} = U_{O,O+\hat{x}+\hat{y}} = U_{O-\hat{x}-\hat{y},O} = -u_{\hat{x}+\hat{y}}, \quad (\text{G16})$$

where the first and the third equation are due to Eq. (G13), and the second is due to Eq. (G15) and the symmetry of the ansatz $U_{ij} = U_{ji}^\dagger$.

Finally we have $u_{\hat{x}+\hat{y}} = u_{\hat{x}-\hat{y}} = 0$.

c. Third neighbor bond

The general form of the third neighbor bonds is:

$$U_{i,i+2\hat{x}} = u_{2\hat{x}}, \quad (\text{G17})$$

$$U_{i,i+2\hat{y}} = u_{2\hat{y}}. \quad (\text{G18})$$

Considering time-reversal transformation \mathcal{T} , we immediately obtain $\{u_{2\hat{x}}, g_{\mathcal{T}}\} = \{u_{2\hat{y}}, g_{\mathcal{T}}\} = 0$. Considering reflection P_y , we have $[u_{2\hat{x}}, g_{P_y}] = [u_{2\hat{y}}, g_{P_y}] = 0$. And under reflection P_{xy} , we have $u_{2\hat{y}} = i \tau_1 u_{2\hat{x}} (i \tau_1)^\dagger$.

Therefore we have $u_{2\hat{x}} = u_{2\hat{y}} = \chi \tau_1$.

d. Fourth neighbor bond

The fourth neighbor is required to obtain a Z_2 spin liquid. The general form of the fourth neighbor is

$$U_{i,i+2\hat{x}+\hat{y}} = (-)^{ix} u_{2\hat{x}+\hat{y}}, \quad (\text{G19})$$

$$U_{i,i+2\hat{x}-\hat{y}} = (-)^{ix} u_{2\hat{x}-\hat{y}}, \quad (\text{G20})$$

$$U_{i,i+\hat{x}+2\hat{y}} = u_{\hat{x}+2\hat{y}}, \quad (\text{G21})$$

$$U_{i,i+\hat{x}-2\hat{y}} = u_{\hat{x}-2\hat{y}}. \quad (\text{G22})$$

Considering time reversal transformation, we have $[u_{2\hat{x}+\hat{y}}, g_{\mathcal{T}}] = 0$.

For convenience we choose $u_{2\hat{x}+\hat{y}}$ to be $i \gamma \tau_0$, which ensures this state to be a Z_2 spin liquid state. The other bonds can be obtained under reflection P_x, P_y , and P_{xy} . The results are

$$U_{i,i+2\hat{x}+\hat{y}} = (-)^{ix} i \gamma \tau_0, \quad (\text{G23})$$

$$U_{i,i+2\hat{x}-\hat{y}} = -(-)^{ix} i \gamma \tau_0, \quad (\text{G24})$$

$$U_{i,i+\hat{x}+2\hat{y}} = i \gamma \tau_0, \quad (\text{G25})$$

$$U_{i,i+\hat{x}-2\hat{y}} = -i \gamma \tau_0. \quad (\text{G26})$$

In conclusion, the symmetry allowed ansatz for the $Z_2 B \tau_-^1 \tau_-^1 \tau_-^1 \tau_-^3$ state are

$$U_{i,i+\hat{x}} = \eta \tau_3, \quad (\text{G27})$$

$$U_{i,i+\hat{y}} = -(-)^{ix} \eta \tau_3, \quad (\text{G28})$$

$$U_{i,i+2\hat{x}} = U_{i,i+2\hat{y}} = \chi \tau_1, \quad (\text{G29})$$

$$U_{i,i+2\hat{x}+\hat{y}} = (-)^{ix} i \gamma \tau_0, \quad (\text{G30})$$

$$U_{i,i+2\hat{x}-\hat{y}} = -(-)^{ix} i \gamma \tau_0, \quad (\text{G31})$$

$$U_{i,i+\hat{x}+2\hat{y}} = i \gamma \tau_0, \quad (\text{G32})$$

$$U_{i,i+\hat{x}-2\hat{y}} = -i \gamma \tau_0, \quad (\text{G33})$$

$$a_0^1 \neq 0. \quad (\text{G34})$$

After Fourier transformation, the Hamiltonian becomes $H = \Psi_{\mathbf{k}}^\dagger M \Psi_{\mathbf{k}}$, where

$$M = 2\eta\cos(k_x)\Gamma_1 - 2\eta\cos(k_y)\Gamma_2 \quad (\text{G35})$$

$$+ \{a_0^1 + 2\chi[\cos(2k_x) + \cos(2k_y)]\}\Gamma_3 \quad (\text{G36})$$

$$+ 2\gamma[\sin(k_x + 2k_y) - \sin(k_x - 2k_y)]\Gamma_4 \quad (\text{G37})$$

$$+ 2\gamma[\sin(2k_x + k_y) - \sin(2k_x - k_y)]\Gamma_5, \quad (\text{G38})$$

where η , χ , γ are all real numbers, and we have used the Nambu spinor representation

$$\Psi_{\mathbf{k}} = (f_{u\mathbf{k}\uparrow}, f_{v\mathbf{k}\uparrow}, f_{u-\mathbf{k}\uparrow}^\dagger, f_{v-\mathbf{k}\downarrow}^\dagger)^T, \quad (\text{G39})$$

and

$$\Gamma_1 = \tau_3 \otimes \tau_1, \quad (\text{G40})$$

$$\Gamma_2 = \tau_3 \otimes \tau_3, \quad (\text{G41})$$

$$\Gamma_3 = \tau_1 \otimes \tau_0, \quad (\text{G42})$$

$$\Gamma_4 = \tau_0 \otimes \tau_1, \quad (\text{G43})$$

$$\Gamma_5 = \tau_0 \otimes \tau_3. \quad (\text{G44})$$

Note that $k_x \in (0, \pi)$, $k_y \in (-\pi, \pi)$.

When there is only nearest-neighbor bond present, the state will have two Dirac points at wave-vectors $(k_x, k_y) = (\pi/2, \pm\pi/2)$. By including the Lagrangian multiplier a_0^1 , the third neighbor bond and the fourth neighbor bond, we find that two gaps open at the two Dirac points.

2. Realization of the $Z_2 B \tau_-^2 \tau_-^2 \tau_-^1 \tau_-^3$ state

PSG elements for this state are:

$$G_x(i) = (-)^{i_y} \tau_0; \quad (\text{G45})$$

$$G_y(i) = \tau_0; \quad (\text{G46})$$

$$G_{P_x}(i) = (-)^{i_x+i_y} i \tau_2; \quad (\text{G47})$$

$$G_{P_y}(i) = (-)^{i_x+i_y} i \tau_2; \quad (\text{G48})$$

$$G_{P_{xy}}(i) = (-)^{i_x i_y} i \tau_1; \quad (\text{G49})$$

$$G_{\mathcal{T}}(i) = (-)^{i_x+i_y} i \tau_3. \quad (\text{G50})$$

First, since the term $a_0^l \tau_l$ should be invariant under $G_{\mathcal{T}\mathcal{T}}$, we have $\{a_0^l \tau_l, \tau_3\} = 0$. And it is also invariant under $G_{P_x} P_x$ and $G_{P_{xy}} P_{xy}$, so we have $[a_0^l \tau_l, \tau_1] = [a_0^l \tau_l, \tau_2] = 0$. Hence the Lagrangian multipliers $a_0^{1,2,3} = 0$.

The analysis of the symmetry allowed ansatz is similar to the previous case. A possible ansatz for the realization of a gapped Z_2 spin liquid state is

$$U_{i,i+\hat{x}} = \eta \tau_3, \quad (\text{G51})$$

$$U_{i,i+\hat{y}} = -(-)^{i_x} \eta \tau_3, \quad (\text{G52})$$

$$U_{i,i+2\hat{x}} = \chi \tau_2, \quad (\text{G53})$$

$$U_{i,i+2\hat{y}} = -\chi \tau_2, \quad (\text{G54})$$

$$U_{i,i+2\hat{x}+\hat{y}} = (-)^{i_x} i \gamma \tau_0, \quad (\text{G55})$$

$$U_{i,i+2\hat{x}-\hat{y}} = -(-)^{i_x} i \gamma \tau_0, \quad (\text{G56})$$

$$U_{i,i+\hat{x}+2\hat{y}} = i \gamma \tau_0, \quad (\text{G57})$$

$$U_{i,i+\hat{x}-2\hat{y}} = -i \gamma \tau_0, \quad (\text{G58})$$

$$a_0^{1,2,3} = 0. \quad (\text{G59})$$

After Fourier transformation, the Hamiltonian becomes $H = \Psi_{\mathbf{k}}^\dagger M \Psi_{\mathbf{k}}$, where

$$\begin{aligned} M &= 2\eta\cos(k_x)\Gamma_1 - 2\eta\cos(k_y)\Gamma_2 \\ &+ 2\chi[\cos(2k_x) - \cos(2k_y)]\Gamma_3 \\ &+ 2\gamma[\sin(k_x + 2k_y) - \sin(k_x - 2k_y)]\Gamma_4 \\ &+ 2\gamma[\sin(2k_x + k_y) - \sin(2k_x - k_y)]\Gamma_5, \end{aligned} \quad (\text{G60})$$

where η , χ , γ are all real numbers, and we have used the Nambu spinor representation

$$\Psi_{\mathbf{k}} = (f_{u\mathbf{k}\uparrow}, f_{v\mathbf{k}\uparrow}, f_{u-\mathbf{k}\uparrow}^\dagger, f_{v-\mathbf{k}\downarrow}^\dagger)^T, \quad (\text{G61})$$

and

$$\Gamma_1 = \tau_3 \otimes \tau_1, \quad (\text{G62})$$

$$\Gamma_2 = \tau_3 \otimes \tau_3, \quad (\text{G63})$$

$$\Gamma_3 = \tau_2 \otimes \tau_0, \quad (\text{G64})$$

$$\Gamma_4 = \tau_0 \otimes \tau_1, \quad (\text{G65})$$

$$\Gamma_5 = \tau_0 \otimes \tau_3. \quad (\text{G66})$$

Note that $k_x \in (0, \pi)$, $k_y \in (-\pi, \pi)$. The fourth neighbor bond opens up gaps at two wave-vectors $(k_x, k_y) = (\pi/2, \pm\pi/2)$.

3. Realization of the $Z_2 B \tau_-^1 \tau_-^1 \tau_-^0 \tau_-^3$ state

PSG elements are:

$$G_x(i) = (-)^{i_y} \tau_0; \quad (\text{G67})$$

$$G_y(i) = \tau_0; \quad (\text{G68})$$

$$G_{P_x}(i) = (-)^{i_x+i_y} i \tau_1; \quad (\text{G69})$$

$$G_{P_y}(i) = (-)^{i_x+i_y} i \tau_1; \quad (\text{G70})$$

$$G_{P_{xy}}(i) = (-)^{i_x i_y} \tau_0; \quad (\text{G71})$$

$$G_{\mathcal{T}}(i) = (-)^{i_x+i_y} i \tau_3. \quad (\text{G72})$$

The analysis of the symmetry allowed ansatz is similar to the previous case, hence we will directly show the results here. The next-nearest-neighbor bonds are again prohibited by the symmetry in this case.

The symmetry allowed ansatz for the $Z_2 B \tau_-^1 \tau_-^1 \tau_+^0 \tau_-^3$ state are

$$U_{i,i+\hat{x}} = \eta\tau_3, \quad (\text{G73})$$

$$U_{i,i+\hat{y}} = (-)^{i_y} \eta\tau_3, \quad (\text{G74})$$

$$U_{i,i+2\hat{x}} = u_{i,i+2\hat{y}} = \chi\tau_1, \quad (\text{G75})$$

$$U_{i,i+2\hat{x}+2\hat{y}} = \xi\tau_2, \quad (\text{G76})$$

$$U_{i,i+2\hat{x}-2\hat{y}} = -\xi\tau_2, \quad (\text{G77})$$

$$a_0^1 \neq 0. \quad (\text{G78})$$

After Fourier transformation, the Hamiltonian becomes

$$\begin{aligned} H &= 2\eta\cos(k_x)\Gamma_1 + 2\eta\cos(k_y)\Gamma_2 \\ &+ \{a_0^1 + 2\chi[\cos(2k_x) + \cos(2k_y)]\}\Gamma_3 \\ &+ 2\xi[\cos(2k_x + 2k_y) - \cos(2k_x - 2k_y)]\Gamma_4, \end{aligned} \quad (\text{G79})$$

where $k_x \in (0, \pi)$, $k_y \in (\pi, \pi)$, and

$$\Gamma_1 = \tau_3 \otimes \tau_1, \quad (\text{G80})$$

$$\Gamma_2 = \tau_3 \otimes \tau_3, \quad (\text{G81})$$

$$\Gamma_3 = \tau_1 \otimes \tau_0, \quad (\text{G82})$$

$$\Gamma_4 = \tau_2 \otimes \tau_0. \quad (\text{G83})$$

The Lagrangian multiplier a_0^1 and the third neighbor bond open up gaps at the two Dirac points $(k_x, k_y) = (\pi/2, \pm\pi/2)$.

4. Realization of the $Z_2 A \tau_-^1 \tau_-^1 \tau_+^0 \tau_+^3$ state

PSG elements are:

$$G_x(i) = G_y(i) = \tau_0; \quad (\text{G84})$$

$$G_{P_x}(i) = (-)^{i_x+i_y} i\tau_1; \quad (\text{G85})$$

$$G_{P_y}(i) = (-)^{i_x+i_y} i\tau_1; \quad (\text{G86})$$

$$G_{P_{xy}}(i) = \tau_0; \quad (\text{G87})$$

$$G_{\mathcal{T}}(i) = i\tau_3. \quad (\text{G88})$$

First, since the term $a_0^1 \tau_l$ should be invariant under $G_{\mathcal{T}}$, we have $\{a_0^1 \tau_l, \tau_3\} = 0$. And it is also invariant under $G_{P_x} P_x, G_{P_y} P_y$ and $G_{P_{xy}} P_{xy}$, so $[a_0^1 \tau_l, \tau_1] = 0$. Hence we have $a_0^1 \neq 0$ and $a_0^{2,3} = 0$.

a. Nearest-neighbor bond

In this state, the gauge transformation $G_x, G_y, G_{P_{xy}}$ are trivial, we can simply write down the general form of the nearest bond:

$$U_{i,i+\hat{x}} = U_{i,i+\hat{y}} = u_{\hat{x}}. \quad (\text{G89})$$

The bond $u_{\hat{x}}$ is invariant under time-reversal transformation, therefore we have $G_{\mathcal{T}}(i)u_{\hat{x}}G_{\mathcal{T}}(i+\hat{x})^\dagger = -u_{\hat{x}}$, which leads to $\{u_{\hat{x}}, \tau_3\} = 0$.

$u_{\hat{x}}$ is also invariant under P_y , therefore we have $G_{P_y}u_{\hat{x}}G_{P_y}^\dagger = u_{\hat{x}}$, which leads to $\{u_{\hat{x}}, \tau_1\} = 0$.

In conclusion, the nearest bonds are as follows:

$$U_{i,i+\hat{x}} = U_{i,i+\hat{y}} = \eta\tau_2. \quad (\text{G90})$$

b. Next-nearest-neighbor bond

The general form of the next-nearest bonds are

$$U_{i,i+\hat{x}+\hat{y}} = u_{\hat{x}+\hat{y}}, \quad (\text{G91})$$

$$U_{i,i+\hat{x}-\hat{y}} = u_{\hat{x}-\hat{y}}. \quad (\text{G92})$$

The bond is invariant under time-reversal operation, therefore we have $G_{\mathcal{T}}u_{\hat{x}+\hat{y}}G_{\mathcal{T}}^\dagger = u_{\hat{x}+\hat{y}}$, which leads to $\{u_{\hat{x}+\hat{y}}, \tau_3\} = 0$. Thus we can choose $u_{\hat{x}+\hat{y}}$ to be $\chi\tau_1 + \xi\tau_2$. And from G_{P_y} , we can obtain $u_{\hat{x}-\hat{y}} = \chi\tau_1 - \xi\tau_2$.

c. Third neighbor bond

Since the $G_x, G_y, G_{P_{xy}}$ are trivial, we have

$$U_{i,i+2\hat{x}} = U_{i,i+2\hat{y}} = u_{2\hat{x}}. \quad (\text{G93})$$

It is invariant under time-reversal transformation, therefore we have $\{u_{2\hat{x}}, \tau_3\} = 0$. It is also invariant under P_y , which leads to $[u_{2\hat{x}}, \tau_1] = 0$. Therefore we have $u_{2\hat{x}} = \zeta\tau_1$. Note that the third neighbor bond is necessary for the *IGG* to be Z_2 .

In conclusion, the ansatz are

$$U_{i,i+\hat{x}} = U_{i,i+\hat{y}} = \eta\tau_2, \quad (\text{G94})$$

$$U_{i,i+\hat{x}+\hat{y}} = \chi\tau_1 + \xi\tau_2, \quad (\text{G95})$$

$$U_{i,i+\hat{x}-\hat{y}} = \chi\tau_1 - \xi\tau_2, \quad (\text{G96})$$

$$U_{i,i+2\hat{x}} = U_{i,i+2\hat{y}} = \zeta\tau_1, \quad (\text{G97})$$

$$a_0^1 \neq 0. \quad (\text{G98})$$

After Fourier transformation, the Hamiltonian becomes $\epsilon_1 \tau_1 + \epsilon_2 \tau_2$, where

$$\epsilon_1 = a_0^1 + 2\zeta[\cos(2k_x) + \cos(2k_y)] + 4\chi\cos(k_x)\cos(k_y), \quad (\text{G99})$$

$$\epsilon_2 = 2\eta[\cos(k_x) + \cos(k_y)] - 4\xi\sin(k_x)\sin(k_y). \quad (\text{G100})$$

And the dispersion relation is $E_{\pm} = \pm\sqrt{\epsilon_1^2 + \epsilon_2^2}$, it is easy to see that when a_0^1 is large enough, the spin liquid is gapped.

5. Realization of the $Z_2 A \tau_-^1 \tau_-^1 \tau_+^0 \tau_+^3$ state

PSG elements of this state are:

$$G_x(i) = G_y(i) = \tau_0; \quad (\text{G101})$$

$$G_{P_x}(i) = (-)^{i_x+i_y} i\tau_1; \quad (\text{G102})$$

$$G_{P_y}(i) = (-)^{i_x+i_y} i\tau_1; \quad (\text{G103})$$

$$G_{P_{xy}}(i) = \tau_0; \quad (\text{G104})$$

$$G_{\mathcal{T}}(i) = (-)^{i_x+i_y} i\tau_3. \quad (\text{G105})$$

The analyze of this state is in much the same way as that of the $Z_2 A \tau_+^1 \tau_-^1 \tau_+^0 \tau_-^3$ case, here we will only show the results:

$$U_{i,i+\hat{x}} = U_{i,i+\hat{y}} = \eta \tau_3, \quad (\text{G106})$$

$$U_{i,i+\hat{x}+\hat{y}} = \chi \tau_1 + \xi \tau_2, \quad (\text{G107})$$

$$U_{i,i+\hat{x}-\hat{y}} = \chi \tau_1 - \xi \tau_2, \quad (\text{G108})$$

$$U_{i,i+2\hat{x}} = U_{i,i+2\hat{y}} = \zeta \tau_1, \quad (\text{G109})$$

$$a_0^1 \neq 0. \quad (\text{G110})$$

The mean-field Hamiltonian is $\epsilon_1 \tau_1 + \epsilon_2 \tau_2 + \epsilon_3 \tau_3$, where

$$\epsilon_1 = a_0^1 + 2\zeta[\cos(2k_x) + \cos(2k_y)] + 4\chi \cos(k_x) \cos(k_y), \quad (\text{G111})$$

$$\epsilon_2 = -4\xi \sin(k_x) \sin(k_y), \quad (\text{G112})$$

$$\epsilon_3 = 2\eta[\cos(k_x) + \cos(k_y)]. \quad (\text{G113})$$

The energy dispersion is $E_{\pm} = \pm \sqrt{\epsilon_1^2 + \epsilon_2^2 + \epsilon_3^2}$. When a_0^1 is sufficiently large, the dispersion is necessarily gapped.

6. Realization of the $Z_2 A \tau_+^0 \tau_-^0 \tau_+^0 \tau_-^3$ state

PSG elements are:

$$G_x(i) = G_y(i) = \tau^0, \quad (\text{G114})$$

$$G_{P_x}(i) = G_{P_y}(i) = G_{P_{xy}}(i) = \tau^0, \quad (\text{G115})$$

$$G_{\mathcal{T}}(i) = i\tau^3. \quad (\text{G116})$$

The term $a_0^l \tau_l$ is invariant under $G_{\mathcal{T}} \mathcal{T}$, therefore we have $\{a_0^l \tau_l, \tau_3\} = 0$, hence $a_0^{1,2} \neq 0$ and $a_0^3 = 0$.

The gauge transformations $G_x, G_y, G_{P_x}, G_{P_y}, G_{P_{xy}}$ are all trivial, therefore the only constraint comes from time-reversal transformation.

From $G_{\mathcal{T}}(i) u_{ij} G_{\mathcal{T}}(j)^{\dagger} = -u_{ij}$, we have $\{u_{ij}, \tau^3\} = 0$. We can therefore write down a symmetry-allowed ansatz which realizes a gapped Z_2 spin liquid

$$U_{i,i+\hat{x}} = U_{i,i+\hat{y}} = \eta_1 \tau_1 + \eta_2 \tau_2, \quad (\text{G117})$$

$$U_{i,i+\hat{x}\pm\hat{y}} = \chi \tau_1, \quad (\text{G118})$$

$$U_{i,i+2\hat{x}} = U_{i,i+2\hat{y}} = \xi \tau_2, \quad (\text{G119})$$

$$a_0^{1,2} \neq 0. \quad (\text{G120})$$

The mean-field Hamiltonian is $\epsilon_1 \tau_1 + \epsilon_2 \tau_2$, where

$$\epsilon_1 = a_0^1 + 2\eta_1[\cos(k_x) + \cos(k_y)] + 4\chi \cos(k_x) \cos(k_y), \quad (\text{G121})$$

$$\epsilon_2 = a_0^2 + 2\eta_2[\cos(k_x) + \cos(k_y)] + 2\xi[\cos(2k_x) + \cos(2k_y)]. \quad (\text{G122})$$

The dispersion relation is $E_{\pm} = \pm \sqrt{\epsilon_1^2 + \epsilon_2^2}$. When a_0^1, a_0^2 are sufficiently large, the dispersion is necessarily gapped.

7. Realization of the $Z_2 A \tau_+^0 \tau_-^0 \tau_+^0 \tau_-^0$ state

PSG elements are:

$$G_x(i) = G_y(i) = \tau^0, \quad (\text{G123})$$

$$G_{P_x}(i) = G_{P_y}(i) = G_{P_{xy}}(i) = \tau^0, \quad (\text{G124})$$

$$G_{\mathcal{T}}(i) = (-)^{i_x+i_y} \tau^0. \quad (\text{G125})$$

We can prove that this state is necessarily gapless which is protected by the PSG symmetry⁵¹. Since G_x and G_y are trivial, the mean-field ansatz is manifestly translational invariant, therefore we can write down the mean-field Hamiltonian as

$$H(\mathbf{k}) = \epsilon^{\mu}(\mathbf{k}) \tau_{\mu}, \quad (\text{G126})$$

where $\mu = 1, 2, 3$.

The condition $G_{\mathcal{T}}(i) u_{ij} G_{\mathcal{T}}(j)^{\dagger} = -u_{ij}$, when translated into \mathbf{k} space, becomes $g_{\mathcal{T}} H(k_x, k_y) g_{\mathcal{T}}^{\dagger} = -H(k_x + \pi, k_y + \pi)$, $g_{\mathcal{T}} = \tau_0$. Therefore we have

$$\epsilon^{\mu}(k_x, k_y) = -\epsilon^{\mu}(k_x + \pi, k_y + \pi). \quad (\text{G127})$$

And from $G_{P_{xy}} H(k_x, k_y) G_{P_{xy}}^{\dagger} = H(k_y, k_x)$ we have

$$\epsilon^{\mu}(k_x, k_y) = \epsilon^{\mu}(k_y, k_x), \quad (\text{G128})$$

Eq. (G127) and Eq. (G128) indicate that the Hamiltonian is gapless along the line $(k_x, k_x + \pi)$. On the one hand, we have $\epsilon^{\mu}(k_x, k_x + \pi) = -\epsilon^{\mu}(k_x + \pi, k_x)$ from Eq. (G127). On the other hand, we have $\epsilon^{\mu}(k_x, k_x + \pi) = \epsilon^{\mu}(k_x + \pi, k_x)$ from Eq. (G128). Therefore $\epsilon^{\mu}(k_x, k_x + \pi)$ must vanish for any k_x , indicating that the Hamiltonian is gapless along this line. Similarly, we can prove that the Hamiltonian is gapless along the line $(k_x, \pi - k_x)$. Thus, we have completed our proof that the $Z_2 A \tau_+^0 \tau_-^0 \tau_+^0 \tau_-^0$ state is necessarily gapless.

8. Realization of the $Z_2 A \tau_+^0 \tau_-^0 \tau_+^0 \tau_-^3$ state

PSG elements are:

$$G_x(i) = G_y(i) = G_{P_x}(i) = G_{P_y}(i) = G_{P_{xy}}(i) = \tau^0, \quad (\text{G129})$$

$$G_{\mathcal{T}}(i) = (-)^{i_x+i_y} i\tau^3. \quad (\text{G130})$$

The term $a_0^l \tau_l$ is invariant under $G_{\mathcal{T}} \mathcal{T}$, therefore we have $\{a_0^l \tau_l, \tau_3\} = 0$, hence $a_0^{1,2} \neq 0$ and $a_0^3 = 0$.

We can label site i with its parity $(-1)^{i_x+i_y}$. Then for a bond u_{ij} connecting even site i with odd site j , we have $[u_{ij}, \tau^3] = 0$. And for a bond u_{ij} connecting two even sites or two odd sites, we have $\{u_{ij}, \tau^3\} = 0$. Since u_{ij} becomes u_{ji} under $C_4^2 = (P_{xy} P_y)^2$ and translation, we have an additional constraint $u_{ij} = u_{ji} = u_{ij}^{\dagger}$ for any bond u_{ij} .

Therefore we could write down a mean-field ansatz which realizes a gapped Z_2 spin liquid

$$U_{i,i+\hat{x}} = U_{i,i+\hat{y}} = \eta\tau_3, \quad (\text{G131})$$

$$U_{i,i+\hat{x}\hat{y}} = \chi\tau_1, \quad (\text{G132})$$

$$U_{i,i+2\hat{x}} = U_{i,i+2\hat{y}} = \xi\tau_2, \quad (\text{G133})$$

$$a_0^{1,2} \neq 0. \quad (\text{G134})$$

The mean-field Hamiltonian is therefore $\epsilon_1\tau_1 + \epsilon_2\tau_2 +$

$\epsilon_3\tau_3$, where

$$\epsilon_1 = a_0^1 + 4\chi\cos(k_x)\cos(k_y), \quad (\text{G135})$$

$$\epsilon_2 = a_0^2 + 2\xi[\cos(2k_x) + \cos(2k_y)], \quad (\text{G136})$$

$$\epsilon_3 = 2\eta[\cos(k_x) + \cos(k_y)]. \quad (\text{G137})$$

The energy dispersion is $E_{\pm} = \pm\sqrt{\epsilon_1^2 + \epsilon_2^2 + \epsilon_3^2}$. When a_0^1 and a_0^2 are sufficiently large, the dispersion is necessarily gapped.

-
- ¹ P.W. Anderson, Mater. Res. Bull. **8**, 153 (1973).
² L. Balents, Nature **464**, 199 (2010).
³ P.A. Lee, Science **321**, 1306 (2008).
⁴ See e.g. C. Lhullier and G. Misguich, in *Introduction to Frustrated Magnetism*, Springer (2011).
⁵ P.A. Lee, N. Nagaosa, and X.-G. Wen, Rev. Mod. Phys. **78**, 17 (2006).
⁶ M.A. Kastner, R.J. Birgeneau, G. Shirane, and Y. Endoh, Rev. Mod. Phys. **70**, 897 (1998).
⁷ P.J. Hirschfeld, M.M. Korshunov, and I.I. Mazin, Rep. Prog. Phys. **74**, 124508 (2011).
⁸ P. Dai, J. Hu, E. Dagotto, Nat. Phys. **8**, 709 (2012).
⁹ P.W. Anderson, Science **235**, 4793 (1987).
¹⁰ G. Baskaran, arXiv:0804.1341 (unpublished).
¹¹ Y.-Z. You, Z.-Y. Weng, New J. Phys. **16**, 023001 (2014).
¹² A.L. Wysocki, K.D. Belashchenko, and V.P. Antropov, Nat. Phys. **7**, 485 (2011).
¹³ P. Chandra and B. Doucot, Phys. Rev. B **38**, 9335 (1988).
¹⁴ M. P. Gelfand, R. R. P. Singh, and D. A. Huse, Phys. Rev. B **40**, 10801 (1989).
¹⁵ E. Dagotto, and A. Moreo, Phys. Rev. Lett. **63**, 2148 (1989).
¹⁶ F. Figueirido, A. Karlhede, S. Kivelson, S. Sondhi, M. Rocek, and D. S. Rokhsar, Phys. Rev. B **41**, 4619 (1990).
¹⁷ V. N. Kotov, J. Oitmaa, O. P. Sushkov, and Z. Weihong, Phys. Rev. B **60**, 14613 (1999).
¹⁸ L. Capriotti, and S. Sorella, Phys. Rev. Lett. **84**, 3173 (2000).
¹⁹ M. Mambrini, A. Läuchli, D. Poilblanc, and F. Mila, Phys. Rev. B **74**, 144422 (2006).
²⁰ H.C. Jiang, H. Yao, and L. Balents, Phys. Rev. B **86**, 024424 (2012).
²¹ S.-S. Gong, W. Zhu, D.N. Sheng, O.I. Motrunich, and M.P.A. Fisher, Phys. Rev. Lett. **113**, 027201 (2014).
²² N. Read, and S. Sachdev, Phys. Rev. Lett. **66**, 1773 (1991).
²³ X.-G. Wen, Phys. Rev. B **44**, 2664 (1991).
²⁴ S. Sachdev, Phys. Rev. B **45**, 12377 (1992).
²⁵ D.P. Arovas, and A. Auerbach, Phys. Rev. B **38**, 316 (1988).
²⁶ R. Flint, and P. Coleman, Phys. Rev. B **79**, 014424 (2009).
²⁷ X.-G. Wen, Phys. Rev. B **65**, 165113 (2002).
²⁸ Fa Wang, and A. Vishwanath, Phys. Rev. B **74**, 174423 (2006).
²⁹ Tiamhock Tay, and Olexei I. Motrunich, Phys. Rev. B **84**, 020404 (2011).
³⁰ O. Tchernyshyov, R. Moessner, and S. L. Sondhi, Europhys. Lett. **73**, 278 (2006).
³¹ Y.-M. Lu, and Y. Ran, Phys. Rev. B **84**, 024420 (2011).
³² S. V. Isakov, T. Senthil, and Yong Baek Kim, Phys. Rev. B **72**, 174417 (2005).
³³ A. M. Essin, and M. Hermele, Phys. Rev. B **87**, 104406 (2013).
³⁴ Y.-M. Lu, G. Y. Cho, and A. Vishwanath, arXiv:1403.0575.
³⁵ S.-P. Kou, M. Levin, and X.-G. Wen, Phys. Rev. B **78**, 155134 (2008).
³⁶ M. Levin and A. Stern, Phys. Rev. Lett. **103**, 196803 (2009).
³⁷ Y.-M. Lu and A. Vishwanath, arXiv:1302.2634 (2013).
³⁸ Andrej Mesaros and Ying Ran, Phys. Rev. B **87**, 155115 (2013).
³⁹ Y. Qi, and L. Fu, Phys. Rev. B **91**, 100401 (2015).
⁴⁰ R. A. Jalabert and S. Sachdev, Phys. Rev. B **44**, 686 (1991).
⁴¹ S. Sachdev and M. Vojta, J. Phys. Soc. Jpn. **69**, Suppl. B, 1 (2000).
⁴² T. Senthil and M. P. A. Fisher, Phys. Rev. B **62**, 7850 (2000).
⁴³ Y. Huh, M. Punk, and S. Sachdev, Phys. Rev. B **84**, 094419 (2011).
⁴⁴ C. Xu and L. Balents, Phys. Rev. B **84**, 014402 (2011).
⁴⁵ N. Read and S. Sachdev, Int. J. Mod. Phys. B **5**, 219 (1991).
⁴⁶ N. Read and B. Chakraborty, Phys. Rev. B **40**, 7133 (1989).
⁴⁷ S. Yunoki and S. Sorella, Phys. Rev. B **74**, 014408 (2006).
⁴⁸ Fan Yang and Hong Yao, Phys. Rev. L **109**, 147209 (2012).
⁴⁹ Tao Li, Federico Becca, Wenjun Hu, and Sandro Sorella, Phys. Rev. B **86**, 075111 (2012).
⁵⁰ B. Dalla Piazza, M. Mourigal, N. B. Christensen, G. J. Nilsen, P. Tregenna-Piggott, T. G. Perring, M. Enderle, D. F. McMorrow, D. A. Ivanov, and H. M. Ronnow, Nat. Phys. **11**, 62 (2015).
⁵¹ X.-G. Wen and A. Zee, Phys. Rev. B **66**, 235110 (2002).